ANL-6610
Reactor Technology
(TID-4500, 17th Ed.)
AEC Research and
Development Report

ARGONNE NATIONAL LABORATORY
9700 South Cass Avenue
Argonne, Illinois

REACTOR DEVELOPMENT PROGRAM PROGRESS REPORT

August 1962

Albert V. Crewe, Laboratory Director

Division	Director
Chemical Engineering	S. Lawroski
Idaho	M. Novick
Metallurgy	F. G. Foote
Reactor Engineering	B. I. Spinrad
Remote Control	R. C. Goertz

- - - -

Report coordinated by R. M. Adams

Issued September 15, 1962

Operated by The University of Chicago
under
Contract W-31-109-eng-38

DISCLAIMER

FOREWORD

The Reactor Development Program Progress Report, issued monthly, is intended to be a means of reporting those items of significant technical progress which have occurred in both the specific reactor projects and the general engineering research and development programs. The report is organized in a way which, it is hoped, gives the clearest, most logical over-all view of progress. The budget classification is followed only in broad outline, and no attempt is made to report separately on each sub-activity number. Further, since the intent is to report only items of significant progress, not all activities are reported each month. In order to issue this report as soon as possible after the end of the month editorial work must necessarily be limited. Also, since this is an informal progress report, the results and data presented should be understood to be preliminary and subject to change unless otherwise stated.

The issuance of these reports is not intended to constitute publication in any sense of the word. Final results either will be submitted for publication in regular professional journals or will be published in the form of ANL topical reports.

The last six reports issued in this series are:

February 1962	ANL-6525
March 1962	ANL-6544
April 1962	ANL-6565
May 1962	ANL-6573
June 1962	ANL-6580
July 1962	ANL-6597

TABLE OF CONTENTS

TABLE OF CONTENTS

TABLE OF CONTENTS

I. WATER COOLED REACTORS

A. EBWR

The construction of additions and modifications to the EBWR plant to permit heat dissipation at power levels up to 100 Mwt has been completed. The plant has recently been authorized to operate up to full power and operational testing at the 40 Mwt level has been reached.

The composition of the current core fuel loading (Core 1A) consists of the following:

Subassembly Type	Number
Spike	32
Natural Uranium (thick plate)	8
Natural Uranium (thin plate)	1
1.44% Enriched (thick plate)	52
1.44% Enriched (thin plate)	54
Total Number of Subassemblies	147

1. Preparation for High Power Operation

a. Reboiler Building Equipment Checkout - A major effort this month was directed to testing the individual components and systems in the new reboiler plant and making nuclear measurements.

In general, the various systems in the reboiler plant are stable in operation and respond well to control. However, certain components (principally valves, pumps, and some instrumentation) require adjustment, replacement or repair.

b. EBWR Transfer Functions - A method has been investigated for determining an analytical expression which represents the best fit to the measured experimental frequency response data. The fitting process is carried out by programming the IBM-704 computer to calculate the amplitude and phase error between an analytical value and the experimental value at each available frequency. The coefficients of a polynomial ratio are adjusted through successive iterations until the error is reduced to a desired minimum. The resulting transfer function then represents a best fit to the available experimental data.

A new approach to the problem of determining reactor transfer functions by direct measurement and calculations was also investigated. The new method involves the use of a periodic reactivity input. If the reactor output were noise free, then a single reactor disturbance would be sufficient. The input reactivity and the neutron flux are sampled simultaneously at fixed intervals of time. The input and output data are fed into

the IBM-704 computer. A computer code is used to compare input and output data and to calculate the coefficients of a transfer function directly from the transient response. In the presence of noise, a periodic input is used, and the resulting sampled values are averaged to reduce the effect of noise. Further analysis is required to determine the relationship between number of transients and desired accuracy as a function of signal to noise ratio. The technique thus far has been investigated by using an analog computer to simulate typical power transfer functions.

2. Experiments

a. Void Coefficient Measurements in Cold EBWR - Void coefficient measurements were made in the EBWR with the insertion of void simulators in up to four thin enriched subassemblies which produced up to 70% void in these elements. The results of these measurements indicated negative void coefficients for the set of conditions indicated below:

Bank Position of Rods Nos. 1-9* (in.)	H_3BO_3 Concentration (gm/gal of water)	$\Delta k/\Delta v$
10.8	0.5	-0.0237
18.3	3.37	-0.0168

*Except No. 2 which was used for obtaining criticality.

These data can be extrapolated to show that a negative void coefficient at criticality bank settings of rods will exist for H_3BO_3 concentrations up to 10 gm/gal in a cold reactor.

b. Power Coefficient Measurements in EBWR - Power coefficient measurements were made in the EBWR (Core 1A) to power levels of 40 Mw, keeping the xenon buildup to a minimum. A nearly constant slope of $\Delta k/\Delta(Mw) \simeq 0.06\%$ was obtained in the 10-40 Mw range. There may actually be some flattening of this slope due to reduced worth of the bank of rods with increasing power or steam void.

Measurements above the 40 Mw level will be made with all rods withdrawn and by varying the concentration of H_3BO_3 in the reactor water in accordance with the criticality requirements.

c. EBWR Neutron Flux Distribution - Spectrum - During a recent period of power operation of the EBWR foil irradiations were made in the tubing loops in the reactor core. Both bare and cadmium-covered foils were used. Radiochemical evaluations of the foils are now being made. This is the first in a series of such irradiations which will be used to characterize the neutron flux in the operating boiling water reactor.

3. Containment Shell Leak Rate Test

A 48-hour building leak rate test was conducted. The test started at 1 p.m. August 4, 1962, and was completed at 1 p.m. August 6, 1962. The leak rate was found to be 2110 ft^3/48 hr (1055 ft^3/day). The allowable leakage is 1000 ft^3/day. This rate includes a leak which developed approximately 46$\frac{3}{4}$ hours after the test was started. Since the leak occurred near the end of the test, the test was considered acceptable. The leak resulted from the movement of sealing compound out of a conduit in the emergency escape hatch. The leak in the conduit was repaired.

B. BORAX-V

1. Operations and Experiments

Cold critical experiments were concluded after finding the optimum oscillator rod arrangement and making flux wire irradiations.

Experiments were performed with various configurations of rotating oscillator rods. The purpose of these experiments was to find a configuration which would yield a large peak-to-peak oscillator worth along with a minimum reduction in available reactivity. Of the three possible positions (reflector, core position 75, and core position 85), core position 75 gave the largest peak-to-peak worth. Table I summarizes the results of experiments in core position 75 with various arc lengths of the poison, changes in water moderator near the poison, and the additional fuel rods near the poison. (A description of the oscillator is given in Section 3.b.)

Table I. Experiments with Rotating Oscillator Rod in Core Position 75

Poison Arc	Rotor Poison	Stator Poison	Peak-to-Peak Worth % Δk/k	Total Worth* % Δk/k	Remarks
165°	Boral, 0.144 in. 50 w/o B_4C	None	0.055	-1.3	Al filler pieces in all 4 corners of oscillator stator
165°	Boral, 0.144 in. 50 w/o B_4C	None	0.047	-1.3	H_2O in 2 corners of stator toward core center
165°	Boral, 0.144 in. 50 w/o B_4C	None	0.074	-1.3	H_2O in 2 corners of stator toward core center
165°	Boral, 0.144 in. 50 w/o B_4C	0.020 in. Cd	0.10	-1.3	Al filler pieces in all 4 corners of oscillator stator
165°	Boral, 0.144 in. 50 w/o B_4C	0.020 in. Cd	0.10	-1.3	H_2O in 2 corners of dummy toward edge of core
60°	0.040 in. Cd	0.040 in. Cd	0.05	-0.8	Al filler pieces in all 4 corners of oscillator stator
90°	0.040 in. Cd	0.040 in. Cd	0.07	-0.8	Al filler pieces in all 4 corners of oscillator stator
165°**	Boral, 0.144 in. 50 w/o B_4C	0.020 in. Cd	0.12	-0.9	Three 5% boiler fuel rods in each corner of stator

*Reactivity effect of substituting the oscillator assembly for a fuel assembly. Rotor and stator poisons adjacent and away from core center line.

**Configuration to be used for transfer function experiments, except stator poison was changed to 0.125 in., 2 w/o Boron-SS.

In order to compensate in part for the loss in reactivity caused by the presence of the oscillator rod, two boron-stainless steel poison rods were removed, one each from core position 66 and 33 (Figure 1).

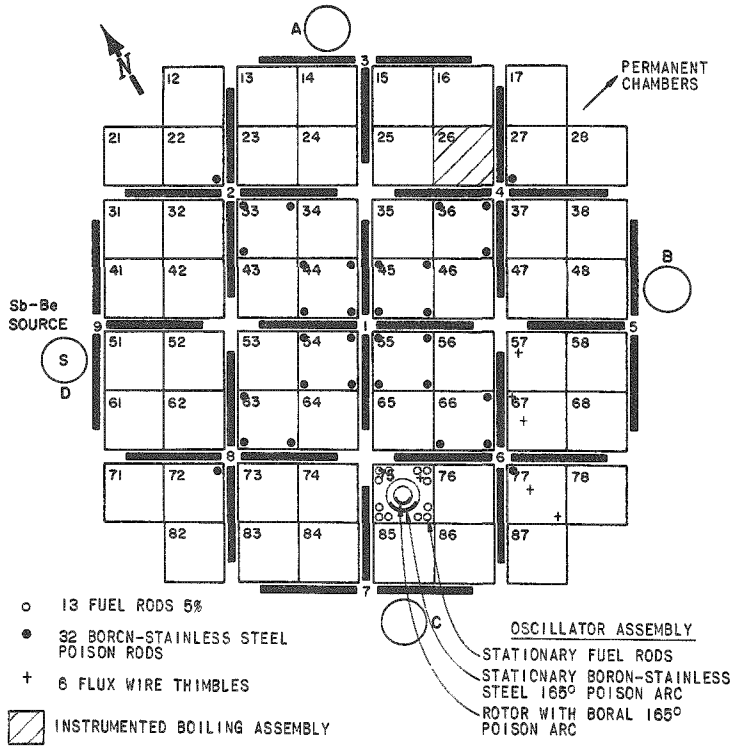

Figure 1. Hot Critical Loading Diagram
BORAX-V Boiling Core

The flux wire irradiations were made to check inconsistent data obtained earlier. These involved five reactor runs to determine overall axial and radial flux distribution, to measure cadmium ratio in aluminum vs. stainless steel holders, to measure control rod flux depression, and to make one check on the effect of varying boric acid concentration. Figure 2 shows typical axial flux distributions for three core locations. Analysis is not sufficiently complete for numerical conclusions on the objectives above. However, the data appear to be very good. A rather large number of $\frac{3}{8}$-in. and 24-in.-long wires of gold and uranium were positioned in axial coolant channels at various radial positions and were irradiated for activation and distribution comparisons.

Preparations were made for operation at 489°F, 600 psig. In-core instrumentation devices were installed. These included six flux wire thimbles in coolant channels and one instrumented boiling assembly (see Figure 1). One hundred twenty-eight (128) void tubes in the central sixteen assemblies and 15 flux wire tubes in coolant channels were installed for the first of the hot critical experiments. The reactor vessel head was installed. Drives for rotating the oscillator rod and raising the source were put into position.

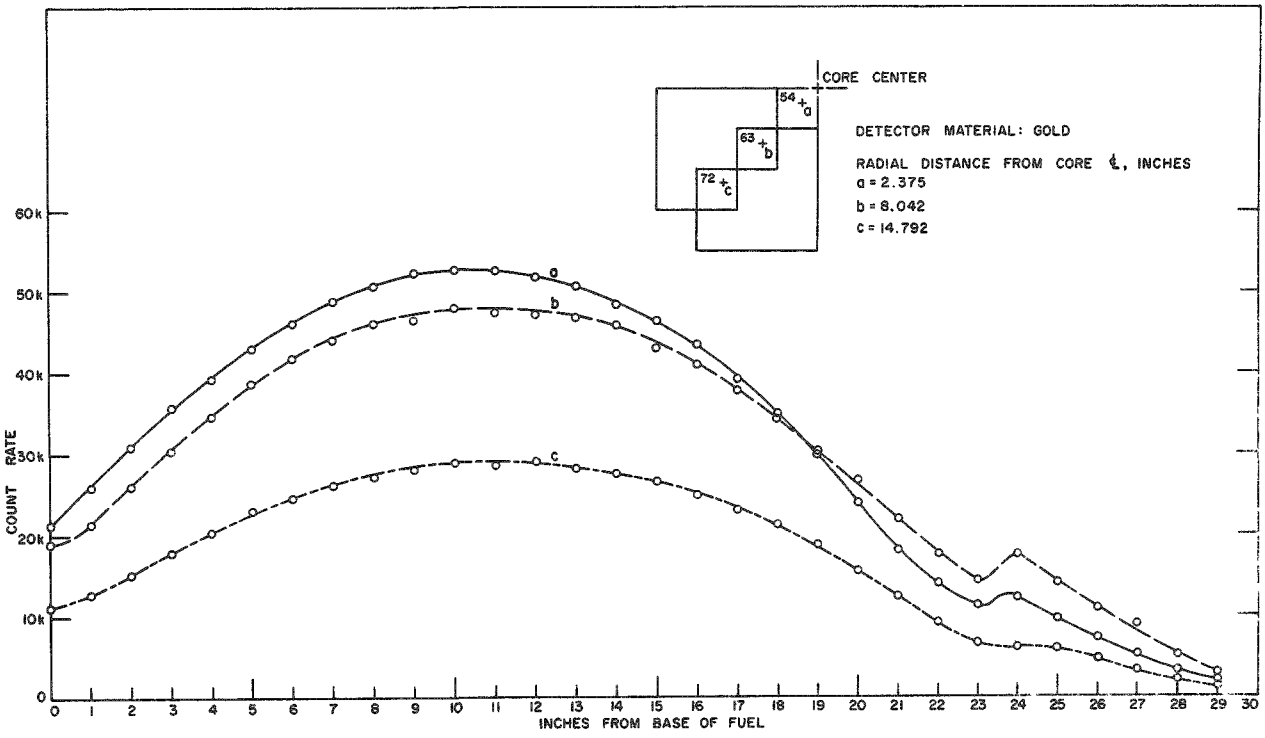

Figure 2. Axial Flux Distribution - BORAX-V

2. Testing and Modification

One of the two 100 hp feedwater pump motors failed after short-time operation. The cause was not proved conclusively, but is believed to be defective winding end connections or moisture. The motor was rewound and put back in service.

As a precautionary measure, the reactor was poisoned with boric acid solution at a concentration of about 20 g/gal (sufficient to maintain the reactor subcritical with all control rods withdrawn). The boric acid addition system was test-operated at zero psig by dumping to drain. Performance was satisfactory.

Replated control rod extension shafts were installed on control rods 4 and 5. Test drops were satisfactory. The old spare extension shaft replating and 1100° heat treating have been completed. The four new spare extension shafts have been ground and are ready for the second heat treatment at 1100°F.

The counting equipment and the continuous wire-counting system were modified and checkout was completed utilizing gold and uranium-aluminum wires irradiated in the AFSR. A study of the gamma decay spectrum of the uranium was made with a 256-channel analyzer to determine optimum counting equipment sensitivity, voltage, and energy

discrimination for counting uranium wires at typical post-irradiation times to be encountered. The results of the study were utilized in the evaluation of wires subsequently irradiated in BORAX-V.

Additional fine flux irradiations were made to determine the effect of a partial substitution of a number of 10%-enriched fuel rods for 5% rods in fuel assemblies near the corners of the core. The results indicated that some power flattening would occur. The effect on reactivity and on the stuck rod criterion of a core the periphery of which was entirely made up in this manner, has not been determined.

3. Critical Experiments

Critical experiments for the BORAX-V central superheater fuel configuration are being performed in the ZPR-VII critical facility.

The measured flooding coefficient of the BORAX-V central superheater was found to be 2.2% ρ in the experimental core. This value was substantially lower than the expected value of 4 to 6%.

The central superheater zone included twelve BORAX-V subassemblies and contained 5.14 kg U^{235}, 0.4 kg U^{238}, about 140 kg Type 304 stainless steel; and about 40 kg H_2O and plexiglas, when voided. The peripheral zone ranged from 1,228 to 1,465 Hi-C fuel elements loaded on a 1.27-cm square lattice. This fuel is present as 3 wt-% enriched uranium, in 0.935 cm diameter UO_2 pellets packaged in aluminum tubing.

The best measurements were made on a critical flooded core. Reactivity was then added by increasing the peripheral (boiling) zone thickness. One or more quadrants of the superheater were voided, and the process was repeated. The reactivity losses from voiding were: first quadrant, 0.47%; diagonally opposite quadrant, 0.42%; remaining two quadrants, 1.3%; and central cruciform sheath, less than 0.01%. The cruciform sheath simulated the central control element follower and metal components of the BORAX-V design.

The control element worths were quite variable, depending upon the thickness of the peripheral fuel zone and upon whether or not the superheater was voided or flooded. Initial control worths had been less than anticipated. Voiding reduced the control element worth by about one-third. Consequently, the five control elements initially provided were supplemented by four five-fingered rods located at the outer edge of the boiling zone.

Preliminary flux distribution measurements indicated nearly equal flux levels in the two fuel regions, with the superheater region voided. With the flooded superheater, however, the flux rose to more than twice the level of that in the boiling zone. Uncorrected bare copper wire activations

gave flux ratios of 1.6 max/min in the radial direction through the voided superheater, and 1.8 max/min when the boiling zone was included. The wire activation at the boiling zone-reflector interface was approximately equal to the highest peak flux in the voided superheater fuel region.

4. Procurement and Fabrication

a. Superheater Fuel - During the month, 25 peripheral subassemblies were brazed. Excessive leakage of argon gas from between side strips and plates of five subassemblies was noted during water immersion leak checking. These were successfully rebrazed. Groups of five subassemblies are welded together with flow vanes into assembly configurations. A total of six such assemblies were completed during the period.

In order to check the effects of the welding operations on the corrosion resistance of the steel, a depleted assembly was fabricated and samples for testing were taken from the welded areas. Samples were subjected to ambient distilled water, and 650°C, 600 psi degassed steam for one week. No detrimental effects were noted.

b. Experimental Components - The rotor of the oscillator assembly (see above, Section 1) is a tube $2\frac{11}{16}$ in. OD and $2\frac{1}{16}$ in. ID, extending the full axial length of the core. The tube is made of 0.144-in.-thick Boral for 165°, with the remainder of aluminum clad with Zircaloy-2. To test the effect of shorter poison arcs, cadmium plate was taped to a $2\frac{5}{8}$-in. OD aluminum tube in arcs of 60° and 90°, extending the full axial core length. The originally designed rotor gave the best results and will be used.

The original stator of the oscillator assembly was a dummy fuel assembly, which is a $3\frac{1}{16}$ in. ID aluminum tube with square end fittings to position it in place of a fuel assembly. Pieces of aluminum were attached to this dummy assembly to fill in the corners, making it effectively a $3\frac{7}{8}$-in.-square bar of aluminum with a $3\frac{1}{16}$ in. ID hole. However, the stator which gave the best results, and the one to be used, was made by altering a spare boiling assembly fuel box. The top and bottom grids were partially removed to make room for the oscillator. Three fuel rod positions were left in each corner. A poison shadow of 2 wt-% boron-stainless steel was installed along one inside wall of the box. Three aluminum filler pieces were installed on the other three inside walls to prevent coolant flow from bypassing the fuel rods.

The equipment for moving a fuel rod past the collimating hole in the fuel rod gamma-scanning system has been designed.

Development work on the Zircaloy-2-to-stainless steel pressure-tight joint is continuing. The third joint fabricated, using pure gold as a braze material, failed the autoclave test. Failure of the gold was worse than the failure of the pure silver joint. A mechanical joint, using a silver-plated stainless steel "O" ring, has been fabricated and is now ready to be tested in the autoclave. Procurement of the remainder of the step-function generator equipment has been canceled until some experiments are completed to determine whether or not it will have sufficient reactivity effect for use at high reactor power.

Two types of sample plates for testing relative reactivity worths of possible substitute control rod materials have been received. They are the Boral plate and the five plates of hafnium.

The repair work on instrumented boiling assembly #1-1 is continuing. Brazing of the splicing sleeves to the extension lead sheaths is complete. Brazing to the old thermocouples is in progress.

Superheater fuel plate thermocouple test-brazing has proceeded. The voids around the thermocouple tips have been reduced. One additional test braze is planned, using a finer-grain, lower-temperature braze material in an effort to eliminate all voids.

Wiring was completed on instrumented boiling fuel assembly #1-2, and the two integral flowmeters (entrance and exit) were calibrated in the BORAX air-water test loop. Both meters were standardized to read inlet water flow rate; and then the exit meter was calibrated for void measurement, using air-water mixtures and the gamma ray attenuation technique. The source and detector were adjusted to measure conditions in the throat of the exit meter, approximately 1 in. upstream from the turbine blades to minimize any errors due to expansion and contraction effects from the fluid.

The assembly is now installed in the reactor vessel, and all circuits have been checked for continuity at the Amphenol connector prior to operation of the reactor system at temperature and pressure.

5. Development and Testing

a. Continuous Chloride Analyzer - The continuous chloride analyzer has been completely checked out for performance and is now ready for use on BORAX-V. The thiocyanate colorimetric method for chloride being used by the continuous analyzer has been adapted for use on a Beckman Model B colorimeter, and standard curves were prepared. The back-up method, using resin, is being investigated and, at present, appears satisfactory. The resin efficiently collects chloride from solutions containing 0.05 ppm, and recovery with ammonium nitrate is complete if a concentrated solution (6 N) is used.

b. Recombiner Tests - Several alternate schemes are being considered for gas generation. Meanwhile, modifications to the test rig are being made.

Thermocouples for monitoring boiler wall temperatures are being installed with provision for heater power to be cut out if excessive temperatures develop. A new test cartridge holder has been constructed, which allows various catalysts to be installed and removed without the mechanical damage caused by the previous design. A constriction inside the body of the boiler for an earlier experiment was causing erroneous water level readings. This is being cut out. Tests for oxygen concentrations have been run on the steam (without gas addition) while the boiler was operating at maximum power, using a modified Winkler method. This method, although quite accurate, requires too large a sample to be useful for this purpose. Therefore, a continuous oxygen analyzer has been installed to sample the condensate stream downstream of the test cartridge. Oxygen concentrations ahead of the test cartridge will be determined by accurate metering. A feedwater and condensate degasser has been installed to insure that oxygen-free feedwater will be injected into the boiler during testing. The difficulty experienced with the test cartridge head-loss D.P. cell has been solved, and piping modifications will be made shortly to prevent further trouble. A low-water-level cutout, which cuts out heater power if the boiler water level drops below the top edge of the strip heaters, has been installed.

Construction work was started on a hot wire-type flowmeter for measurement of injection gas flow rate (if an external gas generator or addition system is used) to the recombiner experiment. The device will use a miniature thermistor bead as the sensing element and is to measure hydrogen and oxygen flow rates in the range of 0-50 cc/min.

c. Advanced Superheater Fuel - A proposal from Atomics International for manufacture of 50 experimental superheater fuel plates, using Type 406 stainless steel cladding, is being considered. Inclusions have been found in the clad-to-clad bond on the developmental plates.

Since AISI Type 406 stainless steel is being considered for test of superheat fuel elements in BORAX-V, development of a brazing procedure for this material is currently in progress. A number of 406 stainless steel (Carpenter Grade 1-JR) plates have been rolled and machined to dimensions corresponding to the superheat fuel dimensions and spacer wires and side strips have been made from this material. A subassembly was made using Coast Metals 60 brazing alloy and procedures identical to those used for the superheat fuel. As was anticipated, grain growth at the brazing temperature (1175°C) was large. In addition the brazing alloy did not wet the steel satisfactorily. The alloy failed to form a consistent fillet and hardened in unevenly distributed areas at or near the lines of application.

Several commercial brazing alloys with lower brazing temperatures are being tried to reduce the grain size in the brazed subassemblies. Since the scale which forms on the Type 406 stainless steel at elevated temperature, even in a vacuum of less than 1×10^{-3} torr, is a likely deterrent to the proper flowing and wetting of the brazing alloys, samples are being thoroughly descaled and plated with 0.0002 in. thick nickel prior to brazing.

d. Superheated Steam Corrosion of Stainless Steel - The preliminary investigation of the effect of surface treatment on corrosion behavior has been extended to other potential structural materials and more carefully controlled experiments have been performed for the stainless steels. These experiments are being performed now so that meaningful corrosion rates may be measured when the new dynamic test facility is completed (1-2 months).

The 300 series stainless steel in oxygenated steam (30 ppm O_2 - 650°C, 600 psi) initially form a temper film on wet ground surfaces. This film transforms in a few days to a much heavier duplex oxide coating. Electropolished samples form the duplex coating almost at once. The same type of heavy coating is formed on electropolished specimens in deoxygenated (0.03 ppm O_2) steam at the same temperature and pressure but the temper film formed on wet ground specimens did not transform duing a one-week exposure. It is tentatively assumed that the temper film is a transient state and corrosion rates measured on electropolished specimens would be more characteristic of the ultimate resistance of the material.

Other possible materials show similar effects of surface preparation. Inco 800 (Incoloy) is quite similar to the 300 SS series. Inco 660 (Inconel), 625, X750 (Inconel X), and AISI 406 show less effect while Rene' 41 is insensitive to surface preparation.

II. LIQUID METAL COOLED REACTORS

A. General Research and Development

1. ZPR-III

The experimental program on Assembly 40, an 8-region, cylindrical reactor, was completed this month. This assembly was designed with a partial-density axial beryllium reflector adjacent to the core and a full-density radial beryllium reflector separated from the core by 9 cm of intermediate reflector. The dimensions and compositions of the various regions were reported in the Progress Report, June, 1962, (ANL-6580).

The radial Be reflector (Zone III of Figure 1, ANL-6580) was withdrawn axially from the reactor in steps. The vacated region was left as void, and the reactivity effect of the blanket motion was measured with respect to this void. Two distinct values of neutron lifetime were obtained from Rossi-α measurements. It is reasoned that neutrons which diffused to the radial Be blanket and back into the core had a measured lifetime about 10 times as long as those remaining within the core proper.

At the conclusion of work with Assembly 40, a number of non-routine checks of the ion chambers were made. These included a calibration, relative to a fixed source in reproducible geometry, as well as a redetermination of plateaus. The instrument response does not indicate any deterioration over the seven-year period that they have been in use.

In addition, the time response of the period amplifiers was measured with a range of ramp and step current inputs. The 15-sec. period trip responded within 30 ms for a large step-function input. For periods down to about 70 ms, the 15-sec. trip responded before two periods had elapsed.

Construction of Assembly 41 is in progress. This is a simulated metallic-fueled, 460-liter core.

2. ZPR-VI and ZPR-IX (Fast Criticals)

a. Building 315 - The control circuits for the emergency venting system and the reactor cell air-conditioning system are being installed. The latter system will be wired to permit operation from the reactor console.

The contract for the installation of the argon gas purge system for the reactor cells has been awarded.

b. ZPR-VI Assembly - Corrections must be made for the sag or displacement of the matrix tubes which occurs when fuel or structure are introduced into the assembly. Tests to determine the magnitude of the displacements are in progress.

Modifications to the dual purpose rod drive mechanisms are in progress. Modification of five of the drives has been completed and they are now being tested through approximately one hundred scram cycles. Upon completion of a successful testing program, the drives will be installed in the facility.

c. ZPR-VI Instrumentation - Modified period and log n amplifiers have been received from the vendor. The performance of these instruments has been tested and appears to meet specifications. The electrometers required in the safety circuits are being made by the Laboratory and will complete the procurement of nuclear instrumentation for the facility.

All ZPR-VI instrument coaxial cables are being checked for noise and continuity.

d. ZPR-VI Experimental Program - A tentative two-year experimental program for ZPR-VI in general terms has been prepared. Other fast reactor programs of interest may also be considered during this period. As currently planned, the operation of the facility will be initiated using an assembly which has been previously investigated but provides margin for improvement and additional measurements. The standard measurements to be made on this and subsequent assemblies will include flux distributions, fission ratios, Rossi-α lifetime determinations, central reactivity coefficients, and spectrum measurements.

The particular objectives of the program, however, will be the investigation of the sodium void coefficient and the Doppler effect in large dilute oxide and carbide systems. Because of the nature of the experiments, the void coefficient measurements will be made first so that the more significant Doppler measurements will result from the second year's activity.

Investigations have shown that the sodium-void coefficient of reactivity becomes less negative and could even become positive in large dilute fast reactors. The magnitude and sign of the effect depends on temperature, core size, and composition. As the size of the core increases, the leakage decreases and any hardening of the spectrum caused by a decrease in sodium density will affect the reactivity.

Since the requirement for a large negative Doppler effect arises from the possibility of a positive or less negative sodium coefficient, it is desirable to verify experimentally the sodium void coefficient as a function of softness of spectrum and spatial dependence.

As rapidly as practical, a large dilute carbide assembly (700 to 1000-liter core) will be built up and its sodium void coefficient measured. The effort will be on a system where theoretical predictions may be checked, rather than on one which might show an unusual effect. From this point, two

basic experimental programs will branch off: a check of the validity of measurements made with a wedge-shaped sodium region in a system containing mostly aluminum mockup elements in place of sodium; and a check on the validity of measuring sodium void coefficients of a large reactor in the central region of a multi-zone reactor. If these techniques can be proven then the investigation of sodium coefficients can be expeditiously performed using cladding material, coolant volume fraction, and enrichment as experimental variables. The alternative to using these generalized methods is of course to make direct measurements for each particular system of interest.

The Doppler effect is an important component of the prompt temperature coefficient of a reactor. The Doppler effect arises from changes in resonance absorption characteristics of core materials with variation in temperature. In large dilute fast reactors with U^{238}/U^{235} or U^{238}/Pu^{239} atomic ratios much greater than unity, it is expected that the Doppler temperature coefficient could be sufficiently negative to enhance the safety of such systems.

Uncertainties in the resonance parameters in the energy region of interest for fissile and fertile materials and in the calculational techniques make it necessary to investigate experimentally the effect in integral measurements.

Some runs to check equipment will probably be made using the hot sample-cold reactor concept. These oscillation experiments will be performed on assemblies constructed for the sodium coefficient program. While these measurements will never be "standard" a sufficient selection will be available for all systems for which the Doppler effect is of interest.

Simultaneously with the experimental program a design study is being made on the feasibility of using a large, heated assembly. In this type of experiment a large heated sample is surrounded by a region which mocks up the gross spectrum. This experiment, when performed, will provide another method for evaluating the magnitude of the Doppler effect.

3. AFSR

During August, AFSR operated to irradiate samples of indium, niobium, molybdenum, and cadmium for the spectral activation investigation. The Nb^{93} $(n,\alpha)Y^{90}$ activation was observed, but no evidence was found of the Nb^{93} (n,n') Nb^{93m} reaction. The irradiation was repeated in EBR-I at much higher intensity, and still no evidence of the second reaction was found. The In^{115} (n,n') In^{115m} was observed and may be a useful indicator. The molybdenum and cadmium data are still being analyzed.

Pilot Scintillator B (a plastic) and anthracene were investigated for their color response to gammas and neutrons. Two approaches were taken; one was to compare counting rate ratios (blue filter to yellow filter), and the

other was based on finding a theoretical counting rate ratio by numerical integration using only transmission characteristics of the photomultiplier, the crystals, and the filters. Results to date encourage further experimentation.

Work continued on the criticality meter. Shop work on the mechanical oscillator was completed, and the oscillator drive mechanism was mounted at the beam hole. However, a preliminary measurement indicated that not enough reactivity effect can be obtained with the beam hole liner in place. On the basis of reactivity measurements made on steel and aluminum with the beam hole liner removed, an oscillator element will be designed.

Work is continuing on the improved period meter. The preamplifier gain is being increased to be compatible with other circuit parameters.

One irradiation of U^{235} and U^{238} foils was performed for inter-Laboratory comparison of counting techniques. Samples were sent to Argonne, Illinois, to Hanford, and to Los Alamos. Consolidated results are not yet available.

The gamma monitoring system in AFSR is being replaced. The new system is designed to use standard Argonne gamma ion chambers. The chambers and components for the electronics have been ordered. An additional limit switch is to be installed on each safety rod to facilitate drop time measurements.

B. EBR-I

1. Mark III Operation

A number of short-term irradiations were performed this month for various Divisions of the Laboratory and for Phillips Petroleum Co.-AED. Generally, they were continuations of series begun earlier and described in the Progress Report for July, 1962.

In conjunction with the irradiations mentioned above, a familiarization and training program was carried out, utilizing trainees from the EBR-II Operating Organization. Four groups have now participated, each for seven days, in the actual operation of EBR-I.

Each group was first given a day of familiarization with the facility. Following this, they took part in interlock and checkout procedures, including calculations of criticality involving temperature coefficient and previous history of the reactor. During the one-week periods, each trainee was allowed to perform a reactor startup under close supervision of a qualified reactor operator.

Trainees also conducted a calibration of control rods and a simulated approach to critical by using the position of the outer blanket to simulate addition of fuel. Further, lectures were given on steady-state and dynamic temperature coefficients, emergency procedures, electromagnetic pump characteristics, and reactor stability.

Modification of the hot cell has been completed, and it is awaiting installation of manipulators.

Inspection of central fuel elements in the core at month's end indicated that their expected increase in diameter has not yet proceeded to the point where they would be difficult to remove. Continued operation with this core while awaiting permission to proceed with the plutonium loading (Mark IV) can, therefore, safely be accomplished.

2. Core IV Fabrication

Processing of the final lot of 0.080 in. O.D. Zircaloy-2 instrument tubing has been completed. The finished tubes are now available for assembly operations.

3. Breeding Gain Specimens

Fabrication of the required 0.005 in. thick discs of both depleted and enriched uranium has been completed. The stainless steel tubing requirements have also been satisfied.

C. EBR-II

1. Reactor Plant

In the Progress Report for July, 1962, (ANL-6597), a brief description was given of the operating difficulty which had arisen with the large rotating plug freeze seal. The dismantling operations subsequently undertaken, the observed damage to the plug seals, and the tentative plans for redesign of the seals were also discussed briefly. In this report a more complete description is provided in each of these areas and the status of the correctional work is brought up to date.

a. Description of Seals - The EBR-II employs two rotating shield plugs as shown in Figure 3. The smaller of the two plugs is located eccentrically within the larger, and mounts a number of mechanisms vital to operation of the reactor. These include the twelve control rod drives, the reactor vessel cover lifting mechanism, holddown mechanism, gripper mechanism, and others. The primary function of the two plugs is to enable positioning the gripper mechanism over any desired point on the reactor for extraction or insertion of a fuel or blanket subassembly. Each plug is

equipped with a "freeze" seal, the purpose of which is to prevent gas leakage into or out of the primary tank around the periphery of the plug. Locations of the seals are indicated in Figure 3.

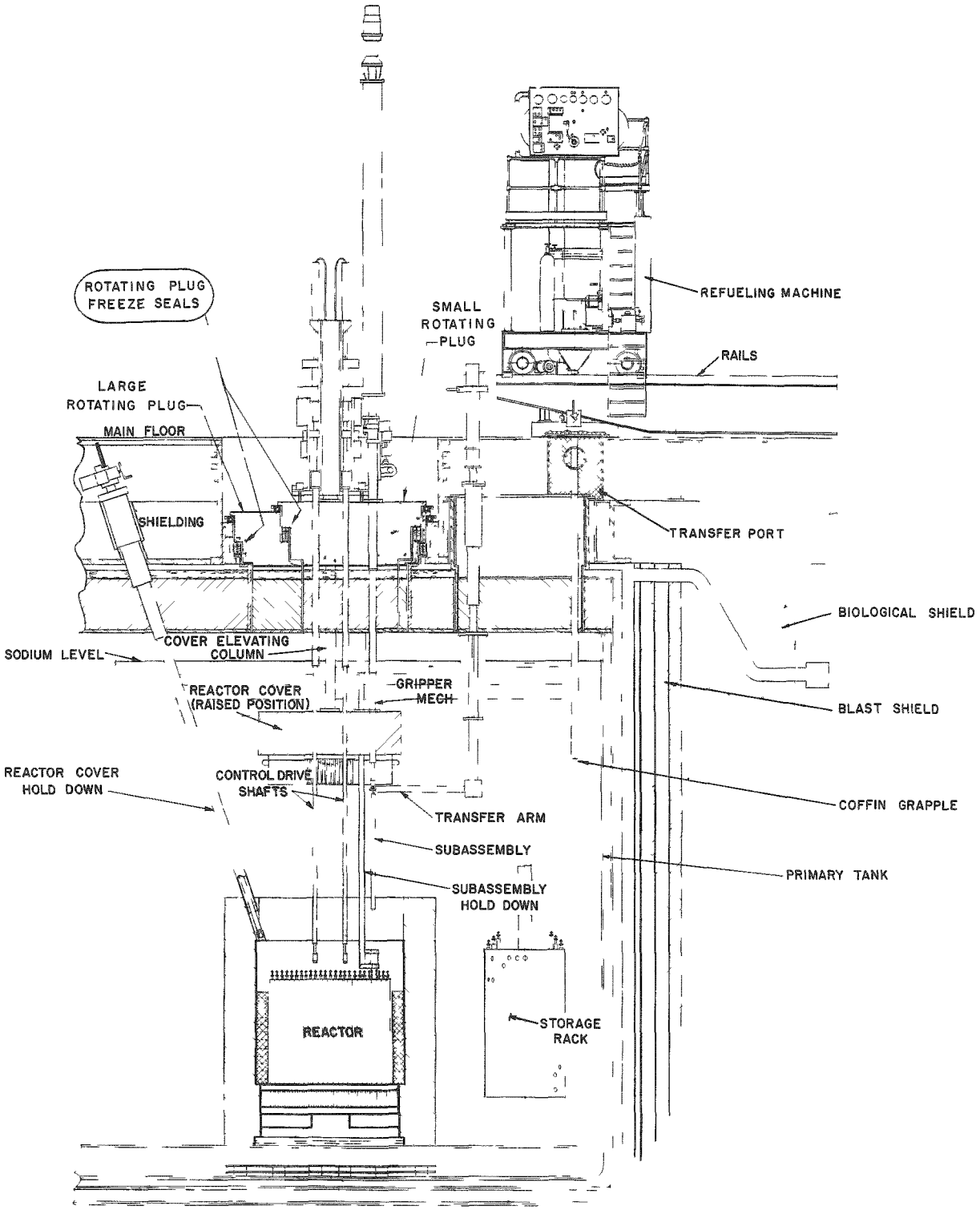

Figure 3. EBR-II Primary System (Showing Location of Rotating Plug Freeze Seals)

Each seal consists of a vertical, cylindrical "blade," or skirt, attached near the periphery of the plug, and a mating annular trough attached to each plug stationary support. The general arrangement is shown in Figure 4.

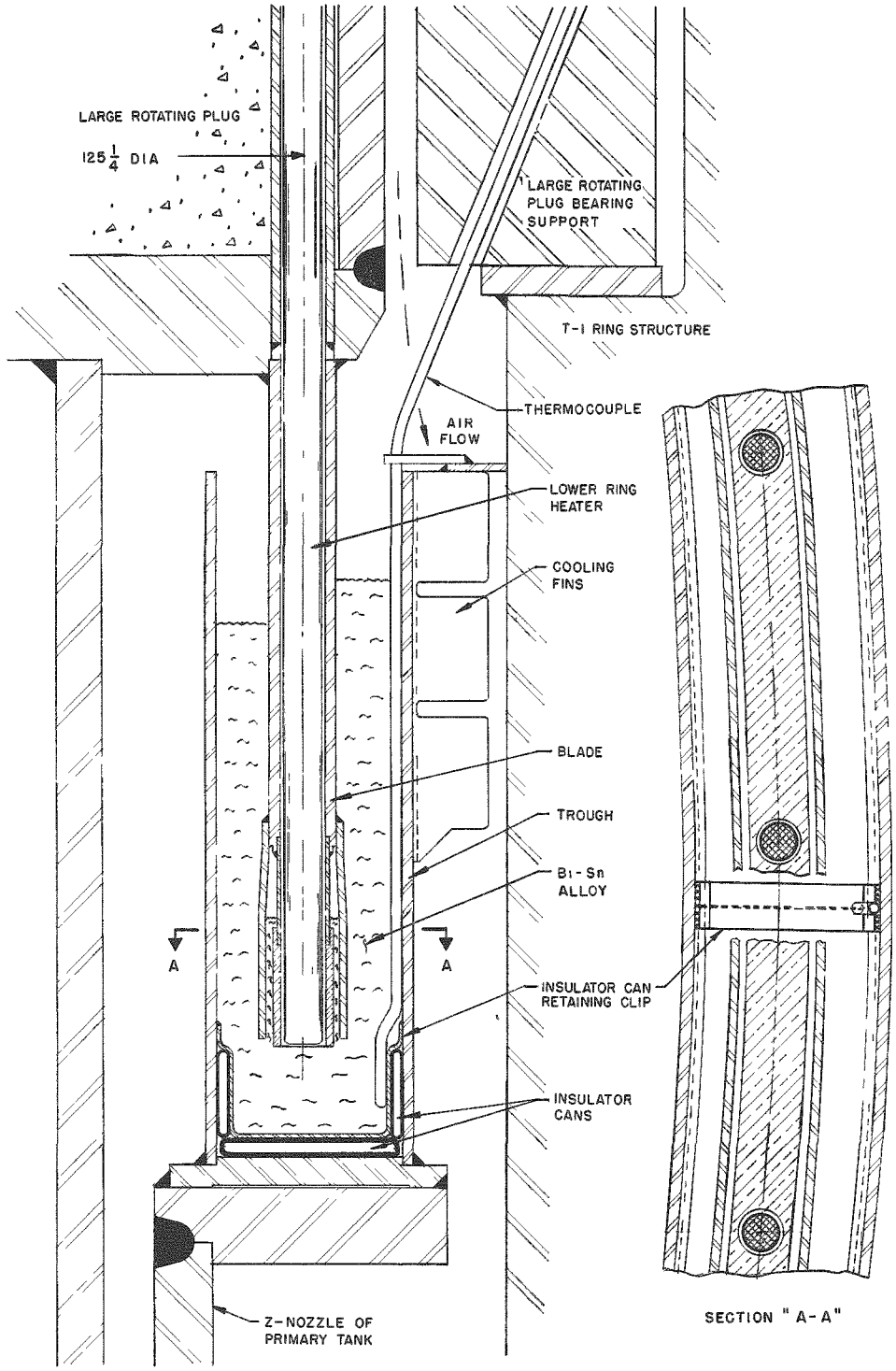

Figure 4. Large Rotating Plug Freeze Seal

As the plug is rotated, the blade rotates within the trough. The trough contains a low-melting-point metal alloy (58% bismuth-42% tin; M.P. 281°F). During plug rotation, as in fuel handling, this alloy is maintained completely molten. During reactor operation, the alloy is maintained frozen at the top but molten at the bottom. Cooling of the seal is effected by flow of air past one side of the trough; cooling fins attached to the upper half of the trough help to maintain a temperature differential between the top and bottom of the trough.

The seal blade is comprised essentially of an upper stainless steel ring and a lower copper ring, with an insulating gas void between the two. The copper ring was incorporated primarily to minimize circumferential thermal gradients. "Fire-Rod" electrical heaters for melting the alloy are located at two different levels within the blade. The heaters at the upper level are used only to heat the seal to the molten condition. Those at the lower level, which are in direct contact with the alloy, are used in maintaining both the molten and the half-frozen conditions. Details of the blade and heater arrangement are shown in Figures 4 and 5.

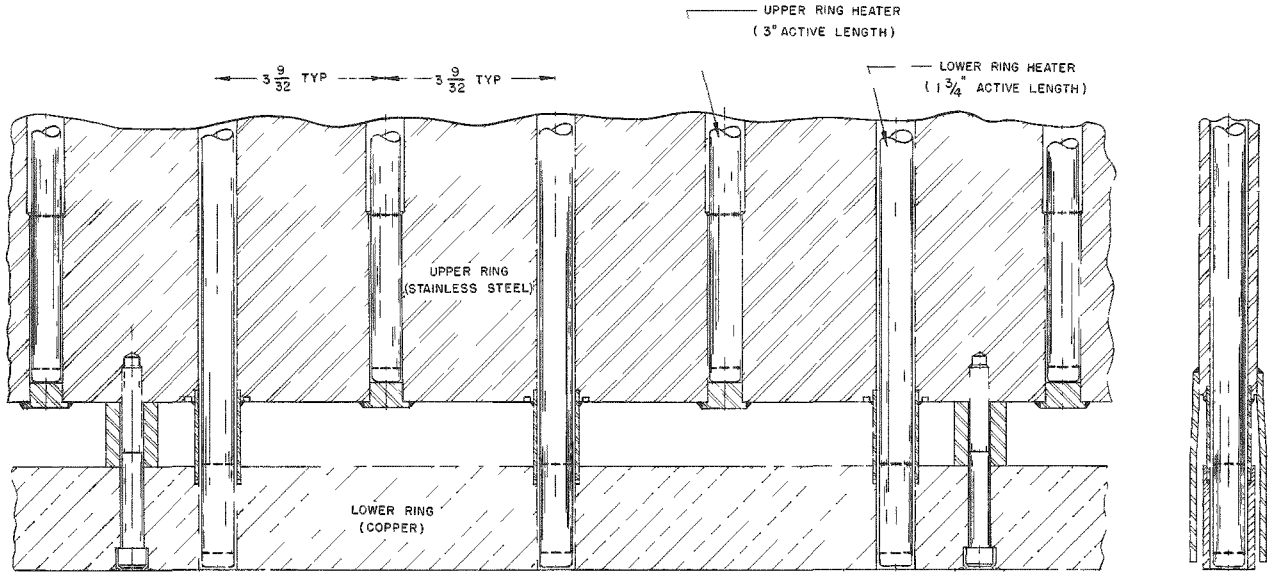

Figure 5. Arrangement of Seal Blade Upper and Lower Rings

b. Description of Operating Difficulty - Prior to installing the main heat exchanger in preparation for filling the primary tank with sodium, a final, comprehensive checkout of the fuel handling system was undertaken. The checkout proceeded smoothly until the first week of July, when difficulty began to be encountered in rotation of the large rotating shield plug. Initially, an occasional "sticking" of the plug with resultant slippage of the clutch on the motor drive unit was noted. This was thought to be caused by excessive thermal expansion of the large ring gear on the plug, resulting in interference with the mating drive gear. The plug had been operating at an abnormally high temperature as a result of several days operation with

the seals molten and with no flow of cooling air. Prior to this time, before filling the seals, the plug had been operated primarily at room temperature. The drive mechanism was therefore loosened, to increase the clearance between the gears. The unit then operated freely, and it was assumed that the cause of sticking had been corrected. Two days later, however, sticking again occurred with similar characteristics. The drive unit was again loosened. The plug then turned, but stuck once more in another position. The drive unit finally was replaced with a manual drive which had been used during original installation. This permitted hand-rotation of the plug, providing some "feel" of the sticking characteristics. It was found that the plug would stick in a non-systematic manner and tended to "bounce" slightly when motion was stopped by the unknown obstruction. This led to the conclusion that a flexible material might be jammed or wedged in one of the clearance spaces and also that the interfering material might move with the plug, accounting for the change in position (angle) where sticking occurred. A possible source of such a flexible obstruction was a heavy-walled rubber hose which had been inserted in the clearance slot between the plug support and the primary tank T-1 structure. This hose had been inserted to close this clearance slot and eliminate bypass air flow in the shield cooling system. It was relatively inaccessible and could not be readily seen except through mirrors and offset viewing devices. Although the hose did not appear to have become dislodged in any way, the decision was made to remove it. The hose eventually was removed with some difficulty, but did not in any way affect the plug sticking characteristics.

In reviewing all the factors relating to the plug sticking, it was decided that the problem might be related directly to the heating of the freeze seal. No definitive mechanism was postulated, but the very long period of successful operation at room temperature seemed to strengthen this possibility. Therefore, the decision was made to drain the bismuth-tin alloy to permit cooling the seal and simultaneously allow rotation of the plug, as rotation is not possible with the seal frozen. Draining of the seal required prior removal of a few lower ring heaters, to provide access to the bottom of the trough. Difficulty in removing the heaters was immediately encountered, and it was discovered that the heaters were bent at their lower extremities. Three were removed, and all were bent at approximately two to four inches from the lower end. Matching the location of the bends with the design of the seal blade led to the conclusion that the lower ring of the blade had become displaced and that the blade had become mechanically jammed in the trough.

On July 11th, draining of the alloy (to a depth of about $\frac{3}{4}$ inch) was accomplished without incident. On July 12th, borescopes were inserted as far as possible into empty heater holes. Although visibility was extremely limited, it was confirmed that portions of the blade lower (copper) ring had become separated from the remainder of the blade and had settled to the bottom of the trough. The need for removing the large plug to permit examination and repair was evident. Because the design of the freeze seal for the small rotating plug is similar to that for the large plug, it was decided to remove both plugs.

c. Description of Dismantling Operations - In preparation for removal of the plugs, it was necessary to dismantle either completely or partially many of the mechanisms installed on them. The reactor vessel cover lifting drive mechanism and superstructure were removed; the lifting columns were left in place on the cover which earlier had been deposited on a temporary support built atop the reactor vessel. The hold-down mechanism was removed, including the drive shaft and funnel. The uppermost portion of the gripper drive mechanism was dismantled, but the lower portion and the drive shaft were left in place. The festoon cables were removed. Shear keys and hold-downs for the two plugs, all wireways which might interfere with lifting of the plugs, and a substantial amount of electrical wiring were removed. Much of the permanent wiring for the freeze seal heaters and thermocouples for the two plugs was replaced with temporary wiring to permit melting (and temperature monitoring) of the residual alloy in the seals at the time of lifting the plugs.

Because dismantling and later reassembly of the twelve control rod drive assemblies would represent a very large additional effort, consideration was given to attempting removal of the small plug with the control rod drives attached. This required that the plug be raised vertically some twenty-one feet with the cover lifting columns sliding through the plug for the entire distance and the control rod drive shafts and gripper drive shaft sliding through their sleeves in the reactor vessel cover for the first seven feet of movement. Because of the small clearances involved, particularly between control rod drive shafts and cover sleeves (0.015 in.), any significant tilting, lateral movement, or rotation of the plug during lifting could be expected to produce binding and serious damage. Detailed examination of possible methods of lifting eventually indicated that such a lift could be accomplished safely. Special lifting fixtures and alignment guides were fabricated and new hoist slings procured. Precision levels were mounted on the plug. Dial indicators for sensing plug lateral motion were installed.

On July 24, after completing all preparations, the small rotating plug was successfully removed and deposited on a newly fabricated support structure in the reactor building basement. On July 27, the large plug was removed without difficulty and placed on the operating floor.

d. Description of Damage - Examination of the large plug seal revealed that severe corrosion had occurred in the lower (copper) ring of the seal "blade." The bismuth-tin alloy had attacked the copper most heavily in the vicinity of the heaters, where the highest temperatures had existed. At these locations the ring was of minimum thickness (see Figure 4) and in numerous places had corroded through, permitting segments of the ring to fall to the seal trough bottom. There the segments caught on projections in the trough (probably retaining clips on the insulator cans) and prevented rotation of the plug. Damage was limited to the lower ring of the seal blade and to some insulator cans positioned within the trough. The upper (stainless steel) ring of the blade and the trough itself were undamaged.

Figure 6 is a view of the large plug seal blade looking upward from underneath. Numerous spaces from which the copper segments had fallen out are evident. A few segments in which bolts happened to be located (see Figure 5) are seen retained in place. The lower ring heaters are also evident (the one extending below the blade bottom was inadvertently pushed there during inspection of the blade). Figure 7 shows the large plug seal trough after removal of the plug. The "crud" at the trough bottom consisted of undrained bismuth-tin alloy and copper. Analysis indicated that this material contained up to 8% copper, while the sound alloy (samples from the alloy drained from both troughs) contained only a few hundred ppm of copper. In Figure 7 a damaged insulator can (trough sidewall) also may be seen. For comparison, Figure 8 shows the empty trough with insulator cans and retaining clips prior to installation of the plug.

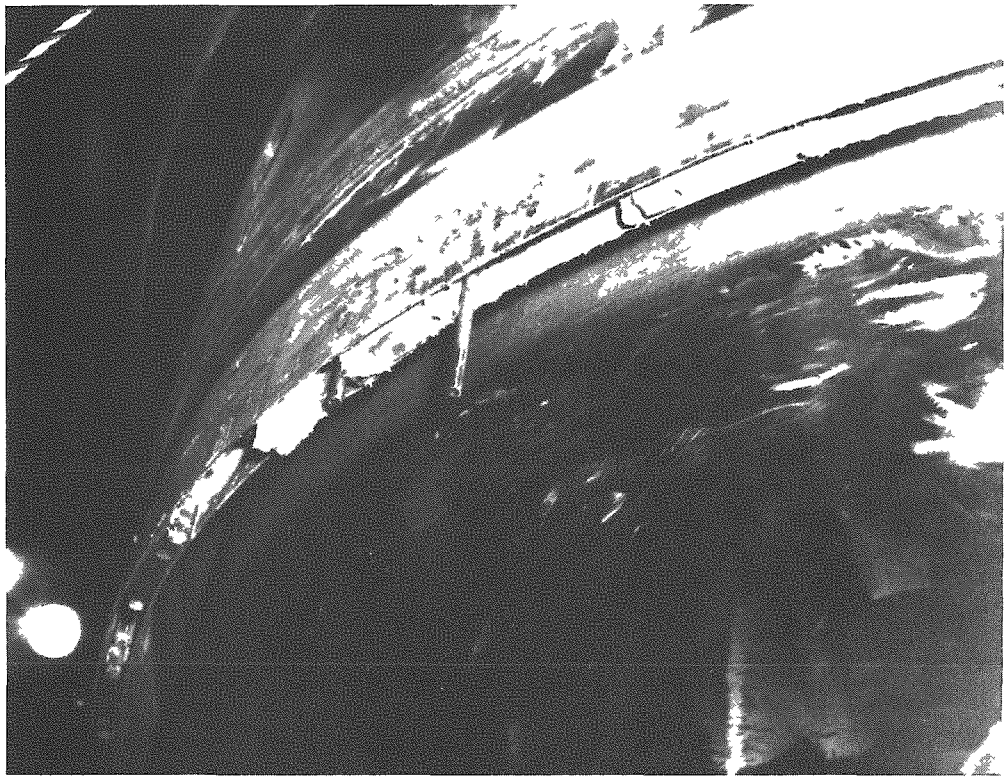

Figure 6. View of Large Rotating Plug Seal Blade after Plug Removal

No physical damage was sustained on the small plug seal except for excessive corrosion of the lower ring of the blade. Although the maximum corrosion again occurred at the heater hole locations, it had not progressed to the same extent as in the large plug seal, and the copper ring (in the original four segments) was intact. Figure 9 shows the ring segments with some of the stainless steel spacers and mounting bolts. The residue in the small plug seal trough, not pictured here, was similar to that in the large plug trough.

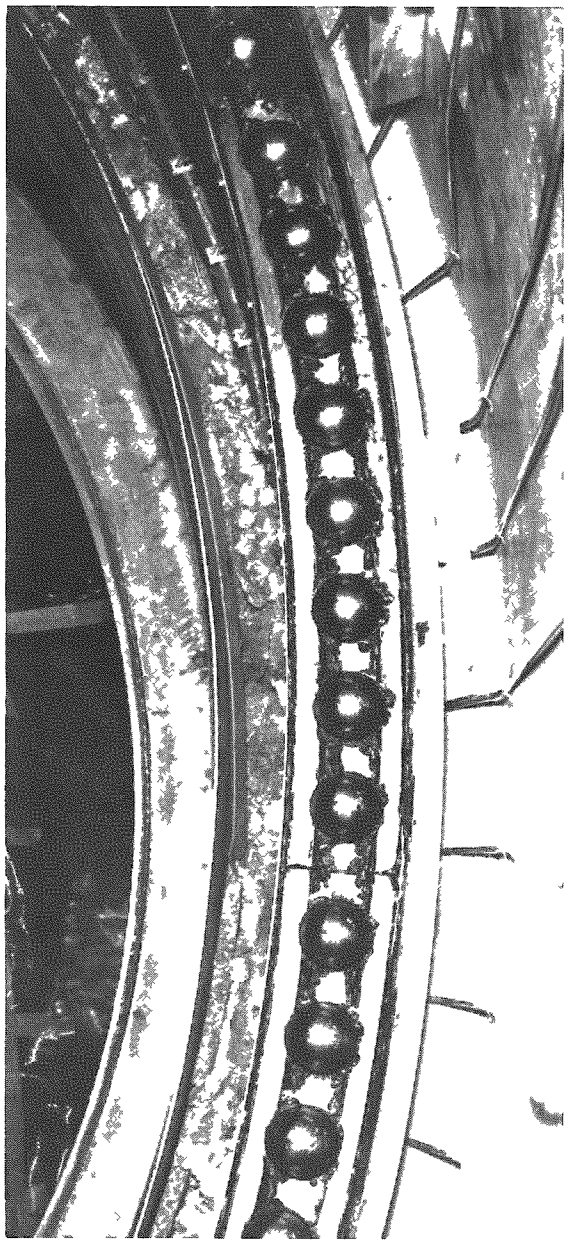

Figure 7. View of Large Rotating Plug Seal Trough after Plug Removal

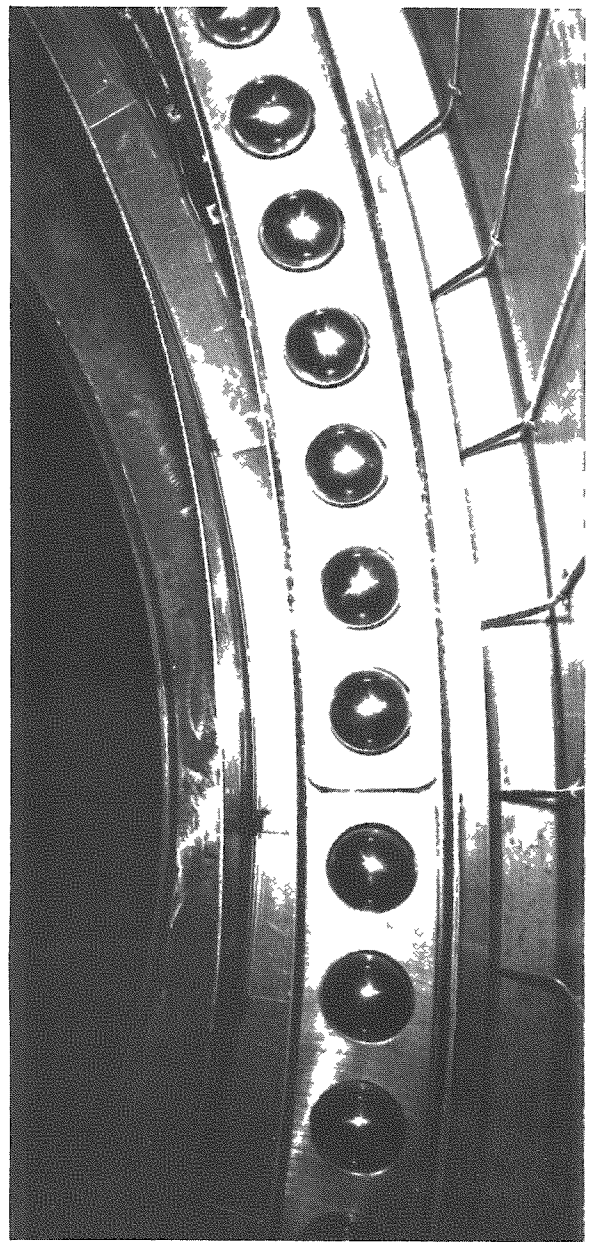

Figure 8. View of Large Rotating Plug Seal Trough before Installation of Plug

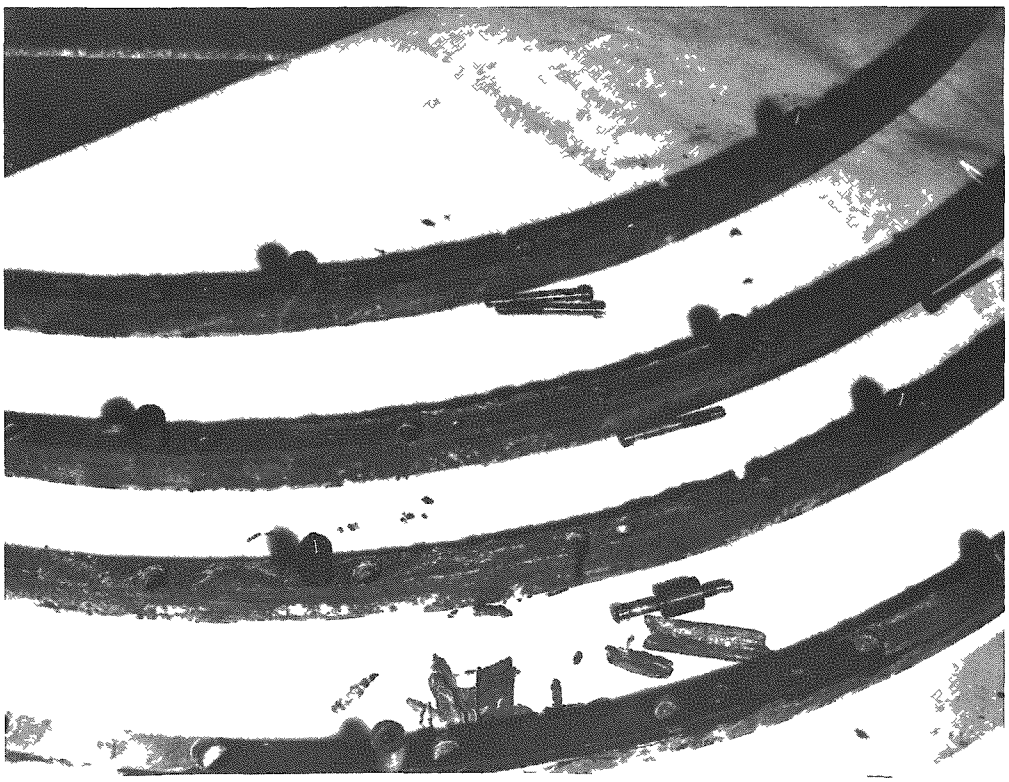

Figure 9. View of Small Rotating Plug Seal Blade Lower (Copper) Ring Segments after Removal from Plug

e. Plans for Correction - The plans for correction are directed at two basic modifications in the seal design and operation: (1) replacement of the copper ring by a stainless steel ring; and (2) minimization of oxidation of the molten seal alloy by operation at minimum practicable temperature and by reduction of the amount of oxygen available to the alloy.

Replacement of the copper ring by a solid stainless steel ring will take the form of an extension to the existing stainless ring to the same depth as the original ring, as shown in Figures 10 and 11. To compensate for the lower thermal conductivity of the stainless ring, the active (heated) zone of each upper heater will be extended downward into the lower ring. This results in a three inch spacing between lower ring heaters, compared to the original six inch spacing.

Operation of the molten alloy at the minimum practicable temperature will be effected by changes designed to provide a temperature distribution as uniform as possible. In addition to extending upper heaters into the lower ring, the active zone of all heaters will be enlarged (upper heaters from 3 in. to $5\frac{1}{2}$ in. length, lower heaters from $1\frac{3}{4}$ in. to $2\frac{1}{2}$ in. length).

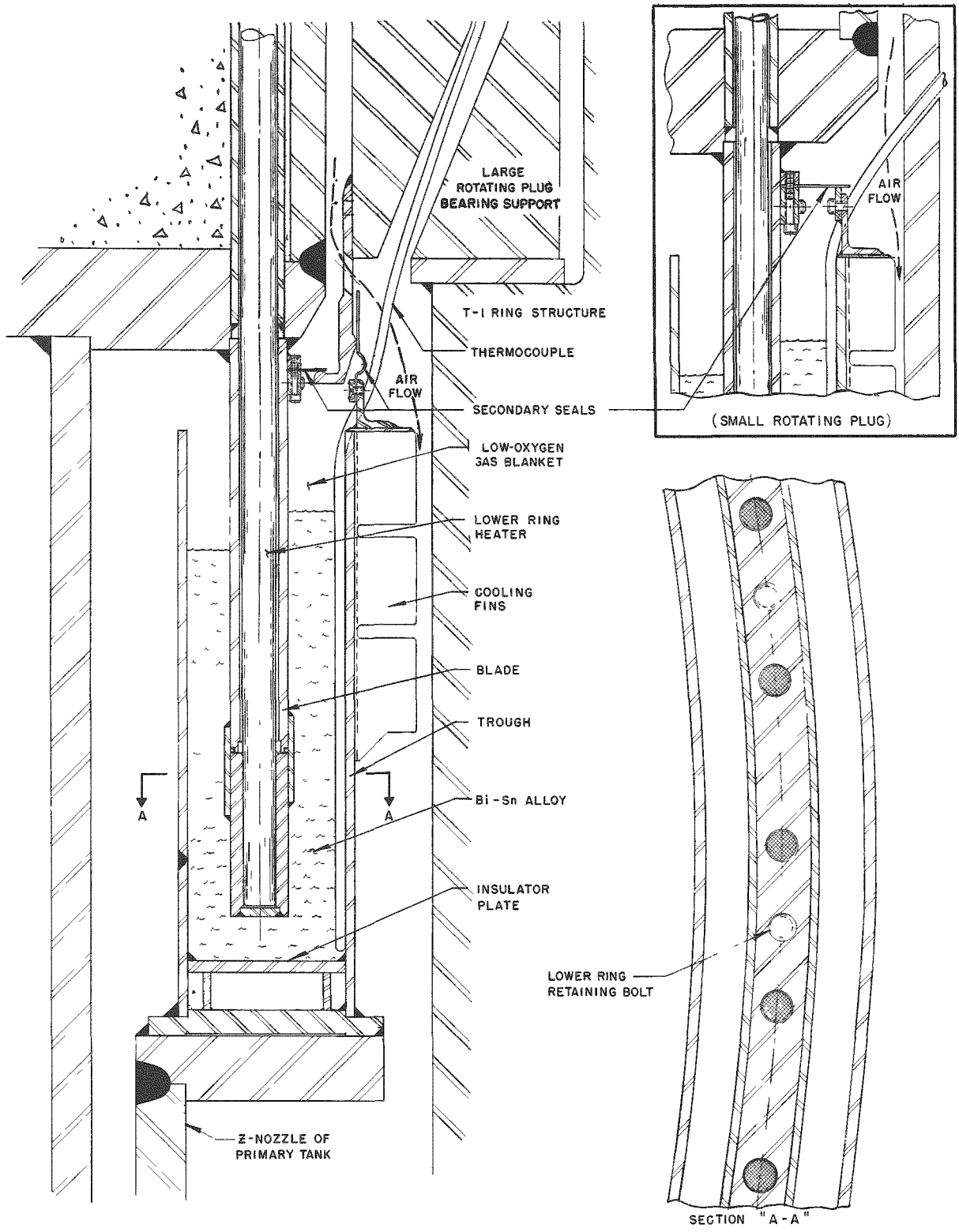

Figure 10. Large Rotating Plug Freeze Seal (Revised)

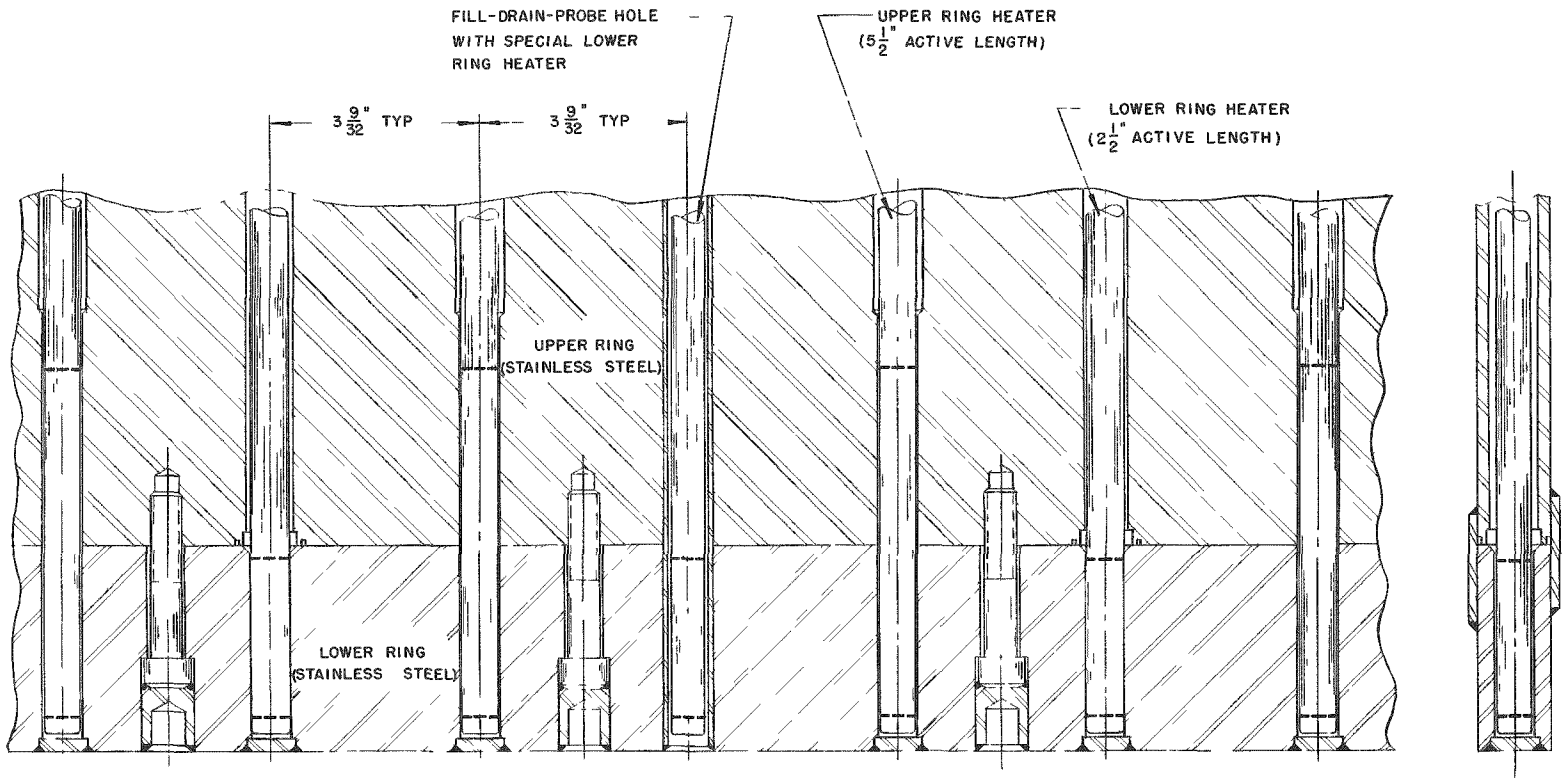

Figure 11. Arrangement of Seal Blade Upper and Lower Rings (Revised)

Thus, the heat sources within the blade will be better distributed and the maximum local heat fluxes reduced. An improved heater control system also will be employed. Formerly, the upper heaters were not energized with the seal in the molten condition; heating was accomplished by the lower heaters only. On-off control was used, all lower heaters being energized or de-energized in unison. Six thermocouples in the seal trough were used for control temperature sensing. A high sensing from any one thermocouple de-energized the heaters, a low sensing from any one energized them. In the new system, both upper and lower heaters will be utilized. The upper heaters will be constantly energized at low power, and the power level may be varied from sector to sector around the seal. On-off control of the lower heaters will again be used, but by sector. The heaters are grouped electricially into six sectors, each sector being controlled individually. Six thermocouples in the seal blade, one per sector, are used for control temperature sensing. During plug rotation, each control thermocouple will bear a constant spatial relationship to the sector of heaters which it controls irrespective of plug position. This improved control system, together with the revised heater arrangement, should permit maintenance of an almost uniform temperature around the seal periphery at the molten alloy surface. This uniformity, in turn, will result in the lowest maximum (local) alloy temperature consistent with assurance that the alloy is fully molten. It is estimated that it will be possible to operate the seal with a maximum temperature of less than 400°F.

Reduction in the amount of oxygen available to the alloy will be effected by providing a low-oxygen, inert gas blanket above the molten seal (on the building atmosphere side only, as the other side is exposed to primary system argon). To maintain such a blanket, a reasonably effective secondary (gas) seal between the rotating plug and the seal trough is required. This seal has proved difficult to design because of the necessity for adapting it to the existing equipment with the attendant space limitations and fabrication and assembly problems. Particularly is this true in the case of the large plug seal. Here the secondary seal must be able to accommodate two types of relative motion: rotation of the plug (or seal blade) in respect to the trough; and, vertical movement between the two. The vertical movement is large, on the order of half an inch; it arises because the trough is mounted on the Z-nozzle of the primary tank, while the plug is mounted on the tank support structure. When the primary tank is heated to 700°F for normal power operation, the center portion of the primary tank cover (to which the Z-nozzle is attached) undergoes downward movement in respect to the support structure because of lengthening of the primary tank hangers and because of bowing, or dishing, of the cover resulting from the normal temperature differential across it.

The design of the large rotating plug secondary seal is shown in Figure 10. In effect, it consists of two separate seals, one to accommodate plug rotation, and the other, the trough movement. It is not expected that a gastight barrier will be effected. To insure against seal failure from

excessive interference, nominal positive clearances are to be provided between mating parts and considerable leakage is anticipated. In operation, an initial flushing of the area above the alloy with inert gas will be accomplished immediately before melting the alloy, followed by a continuous low-flow purge with the inert gas throughout the period in which the alloy is maintained molten. By this means it is expected to be able to maintain a low-oxygen atmosphere over the alloy whenever the alloy is molten and susceptible to oxidation. Laboratory experiments have shown that oxygen concentrations of well below one percent can be achieved.

The secondary seal for the small rotating plug is similar to that for the large plug, but simpler. The trough and plug (or seal blade) do not undergo significant relative vertical motion since both, in effect, are supported by the primary tank support structure. Accordingly, only the single seal for accommodation of rotational movement need be provided, as illustrated in Figure 10. The contemplated manner of operation is the same as for the large plug.

A number of additional improvements to the rotating plug freeze seals or to the plugs themselves have been made possible as a result of removal of the plugs. Based on the seal operating experience already gained, an improved pattern of trough thermocouple locations has been determined and the thermocouples will be repositioned accordingly. In addition, all present thermocouples will be made replaceable so that they may be readily replaced at any time during operation in the future, and some additional, non-replaceable ones installed. The insulator cans at the bottom of the large plug seal trough will be replaced with a continuous insulator plate as shown in Figure 10. This eliminates all mechanical projections at the trough bottom, increases side clearances between trough and blade, and provides a backup weld to insure against leakage of alloy from the trough.

Two "windows" will be provided in each seal to enable viewing of the bismuth-tin alloy surface on either side of the seal blade during operation. It is thought that with the aid of these devices the extent of formation of alloy oxide on the one side or possible accumulation of sodium-sodium oxide on the other can be followed and skimming of the surface can be accomplished, if necessary. The window looking into the building atmosphere side consists of a several-inch-long, rectangular opening cut through the blade wall from one of the upper heater holes. For viewing, the heater in this hole is removed and a borescope inserted. The window looking into the primary system argon side consists of a cylindrical hole drilled vertically through the rotating plug body and capable of accommodating a borescope.

All freeze seal heater holes, both upper and lower, will be dry (except six in each seal located in the fill-drain-probe holes or the window holes). Heaters will no longer be immersed in the seal alloy, thus eliminating the danger of their becoming "soldered in" after heater failure and posing a difficult replacement problem. In addition, the probable frequency of

heater failure, or need for replacement, should be greatly reduced in the future by the lower heat fluxes and the revised control system to be employed.

Several revisions will be made in the air cooling system within the rotating plugs to improve control of the temperature. The ten existing dampers will be reworked to provide a "closed" position and to provide continuous, rather than three-step, adjustment. Two additional dampers will be installed in the two large plug air ducts which formerly had none. Six additional dampers will be installed in the small plug air ducts. Filters will be installed at all air inlets to both plugs. The rubber hose which has been removed from the clearance slot between the large plug support and the primary tank support structure will be replaced with a permanent steel closure.

The bearing seal on each of the rotating plugs will be revised. In the new design a positive-contact, sliding seal employing a resilient ring of organic material in compression against an annular ring of spring steel is used to effect an almost gastight barrier. This arrangement will eliminate the air flow through the bearings which formerly short-circuited a portion of the rotating plug cooling air flow paths, and also will prevent any accumulation of air borne dust in the bearing grease.

f. Present Work Status - The troughs of both seals have been completely cleaned of residual alloy and all original trough thermocouples have been removed. The upper portion of the large plug seal inner trough wall has been cut off to provide access for installation of the trough insulator plate, and this installation has been started. All new (replaceable) thermocouples for the large trough have been readied and their support ring atop the trough cooling fins prepared for their mounting.

The seal blades on both rotating plugs have had the original lower ring removed and the upper ring prepared for installation of the new lower ring. On the large plug, one "window" has been completed (and the other started), and the new lower ring is completed and ready for mounting.

All parts for the secondary seals for both freeze seals have been completed and are on hand in the field. The steel closure replacement for the rubber hose barrier removed from the periphery of the large plug is nearly completed. New heaters, additional electrical components required for the improved heater control system, and additional bismuth-tin alloy have been ordered. Delivery of these items will not cause delay.

Installation of the two new air cooling system dampers in the large rotating plug has been completed. Rework of the ten existing dampers is in progress.

2. Sodium Boiler Plant

Extension of the 2-in. recirculating sodium line in the surge tank was completed. This modification improves sodium circulation in the surge tank.

Immersion heaters were installed in the surge tank. The surge tank level probes, which had been removed for calibration at operating temperature, were reinstalled and wired.

The secondary sodium system was sealed and leak tested successfully with helium.

Installation of conduit, wire, and cable for electrical heating systems and thermocouples was continued. The induction heating system was operated during this period to maintain evaporator and superheater shell temperatures around 200°F, in conjunction with preparations for and performance of chemical cleaning of the steam generator components and associated piping.

Installation of a motor-driven valve operator on the 3-in. feedwater bypass line of the boiler was started. This valve, previously a manually operated valve, is being modified to act as a regulating valve in case of failure of the instrument air supply to the 4-in. pneumatic control valve which normally functions as the feedwater regulating valve.

Insulating work was continued on both indoor and outdoor piping. Insulation of the surge tank was resumed following completion of mechanical work.

Painting of the piping was continued. Coating of the basement floor and wainscot liner was completed.

3. Power Plant

The major job in the Power Plant during this report period was the chemical cleaning of the water sides of the steam generator components and the associated steam and water piping in the Sodium Boiler Plant and in the yard. The initial step in the cleaning operation after heat-up was degreasing of the system surfaces by circulation of a hot (200°F) alkaline detergent solution through the system. Following this treatment an inhibited organic acid formulation at a temperature of about 200°F was circulated through the system for removal of rust and mill scale. Analysis of the cleaning solution showed an iron content equivalent to the dissolution of approximately 458 lb of iron oxide. After the acid solution was drained, the system was thoroughly rinsed for removal of residual solution and was drained for inspection. Observation of the visible steam drum internal surfaces indicated satisfactory removal of adherent mill scale and rust.

Following inspection, the steam generator components and associated piping were filled completely with a sodium chromate corrosion inhibitor solution containing 5000 ppm of chromate ion at a pH of approximately 9.2. According to current plans, the system will remain in wet lay-up, filled with corrosion inhibitor, until the plant is ready for hot operation.

Modification of the cooling tower fan stacks was started to increase the throat diameter, providing greater fan tip clearance, and to provide greater structural strength in the stacks. Sufficient work has been performed on one stack to demonstrate the efficacy of the method. Contingent upon the availability of materials and personnel, this job will be carried to completion prior to the onset of bad weather.

Painting of Power Plant components and pipe lines, in accordance with a color-coding system, was begun during this report period.

4. Fuel Cycle Facility

Corrective work and installation and checking of equipment in the EBR-II Fuel Cycle Facility is continuing.

The control stations for the Argon Cell fuel processing equipment, which are positioned outside the cell windows, have been installed, and the circuitry between the control stations and the subcell is being tested.

The construction of the Interbuilding Coffin, which is being fabricated by a commercial fabricator, is nearly complete. Delivery of the coffin is scheduled for September.

A lifting platform is being designed which will be a part of the transfer cart located in a subcell under the Air Cell. The lifting platform will raise coffins and other containers high enough under an aperture in the Air Cell floor to allow transfer of scrap pails, drums, and equipment into the coffins with a simple manipulator-operated grapple instead of the crane-and-manipulator-operated latching-grapple originally planned.

Adiprene C was tested for use as a gasket material for the large transfer lock. After an exposure of 3×10^9 rad while under compression in a test assembly, Adiprene C was still found to be resilient. It was concluded that Adiprene C was satisfactory for its intended use.

A final inspection of the argon and air cell shielding windows was made jointly with a representative of the vendor. Total window transmission was high (on the order of 16%) and only a few minor mechanical problems were found to remain.

Tests of the cooling capacity of the argon cell refrigeration and circulation system were carried out. With neither of the two cooling boxes was the design efficiency for air temperature reduction quite realized, although the refrigerant compressor rating was achieved. Because it appears that icing of the cooling coils (resulting from moisture in the cell air) was limiting the transfer of heat, further tests will be conducted after drying the cell atmosphere.

Components for the two injection casting furnaces arrived in Idaho and were set up outside the cell. Minor mechanical and electrical changes were made, and it was found necessary to reduce the pallet support height to permit furnace bell placement by manipulator. The interchangeability of spare parts was confirmed. Installation of the furnaces in the argon cell by remote techniques has been started.

In the analytical laboratory, encouraging results have been obtained in tests of a fuel burnup method, potentially useful at low levels, based on mass spectrometric determination of a La^{138}/La^{139} ratio. Lanthanum-138 is added to the fuel solution as a reference standard. Chemical purification is required prior to the lanthanum ratio measurement. In other studies, the application of flame photometry for the determination of individual rare earths in irradiated fissium was investigated. In tests with pure neodymium, a sensitivity to 5 ppm was achieved.

The skull reclamation process requires the mixing of molten metal-salt systems while the systems are held at elevated temperatures. Low frequency inductive heating and mixing is being investigated for this purpose. A skull oxidation run, using 60 cycle power for heating and mixing a magnesium-zinc-flux system achieved a 66 percent reduction of a 2.7-lb skull oxide charge in two hours at 800°C. New equipment is being procured which will allow the power density (and hence the vigor of agitation) to be increased in additional studies of the skull reduction step.

5. Fuel Development

a. Compatibility of Uranium-5 wt-% Fissium with 304 Stainless Steel - Compatibility studies are being made to determine the interaction by solid diffusion between the fuel and clad of the first loading in EBR-II.

A series of heat treatments is being performed on diffusion couples of uranium-5 wt-% fissium alloy with Type 304 stainless steel at 550, 600, 650, and 700°C for one, two, and five weeks. The one and two week heat treatments have been completed and the specimens have been inspected metallographically.

Good bonding was observed on all couples and the total width of the diffusion bands has been measured.

Table II gives the total band widths for one and two weeks at three temperatures. Band formation seems to be about 95% into the uranium and only 5% into the stainless.

Table II. Total Discussion Band Widths (mils) between Uranium-5 wt-% Fissium and 304 Stainless Steel

Temp. (°C)	Band Width (mils)	
	1 wk anneal	2 wk anneal
550	0.75	1.0
600	1.75	2.3
650	3.9	5.3

b. Properties of Uranium-Plutonium-Fissium Alloys - The study of the properties of uranium-plutonium-fissium alloys continues. The thermal conductivity values of the 75 wt-% uranium-20 wt-% plutonium-5 wt-% fissium alloy have been obtained and are listed in Table III. The values are about 8% less than the Core II reference alloy 70 wt-% uranium-20 wt-% plutonium-10 wt-% fissium and almost the same as the 65 wt-% uranium-20 wt-% plutonium-15 wt-% fissium alloy (see July, 1962, Progress Report). Thus, it appears that variations of fissium content from 5 wt-% to 15 wt-% fissium produce little change in the thermal conductivity of the uranium-plutonium-fissium alloys.

Table III. Thermal Conductivity of the 75 wt-% U-20 wt-% Pu-5 wt-% Fs (high zirconium) Alloy

Temp. (°C)	k, cal/sec-cm-°C
200	0.041
300	0.047
400	0.054
500	0.060
600	0.066
700	0.071*

*extrapolated

c. Corrosion of EBR-II Fuel Cladding Materials - In 1960 a program of evaluation of Nb and V base alloys was undertaken to determine their potential use as fuel cladding materials. Part of this program involved a study of their compatibility with liquid sodium. The Nb and V base alloy

samples were exposed to 650°C flowing sodium (about 2 fps) for 504 hours with one (650°C - 20°C) temperature cycle. The Na_2O concentration was maintained at 1-5 ppm using natural uranium as an oxygen getter. The evaluation consisted of weight change measurements and macroscopic observation of the surface.

In order to gain more information on the behavior of the aforementioned alloys a metallographic investigation has been initiated.

The Nb-1.84 wt-% Cr and Nb-4.33 wt-% Zr samples showed no structural changes but exhibited a darker etch in the center of the transverse section than at the edges. Microhardness measurements were taken and these showed the edges to be the hardest, with the hardness decreasing as the center of the specimens were approached. The hardness of the as-received specimens for both alloys was constant across the entire transverse sections.

The hardness in the center of the test specimen was slightly higher than the control for the Nb-Zr alloy and slightly lower than the control for the Nb-Cr specimen. As-received specimens of these two alloys are being annealed in a vacuum at 650°C to see if any change in hardness is due to prolonged time at this temperature irrespective of any corrosion effects.

The Nb-5 wt-% Mo specimen showed no structural changes but the test specimen was slightly softer than the control. It is thought that the softening is due to a stress relief process.

None of the specimens studied to date has shown any evidence of intergranular penetration or substantial surface attack by the Na.

6. Process Development

a. Melt Refining Process Technology - Equipment is being constructed to investigate further the behavior of fission product iodine in the melt refining process. The study will be aimed primarily at obtaining data on the distribution of iodine in the ingot and skull, crucible, and the volatile fraction when inactive and low-activity-level fissium-uranium alloys are melt refined. The alloys will contain cesium and iodine at concentrations expected in discharged EBR-II fuel at two total atom percent burnup.

b. Skull Reclamation Process - To determine optimum process conditions for the skull reclamation process, demonstration runs are being performed on a 130-gram-uranium scale in an argon atmosphere glove box. In previous runs performed in the moisture-free inert atmosphere, poor removals of ruthenium were obtained in the noble metal extraction step. These poor removals are believed to be associated with a loss of

oxidizing power of the flux (47.5 mole percent calcium chloride-47.5 mole percent magnesium chloride-5 mole percent magnesium fluoride) through elimination of reactions with air and water which produce chlorine, hydrogen chloride, and oxychlorides. Similar runs, in which the flux was exposed to air and water, resulted in ruthenium removals of from 75 to 90 percent. In a recently completed experiment in the inert atmosphere glove box, the addition of one weight percent zinc chloride to the flux resulted in a ruthenium removal of 63 percent. This may be compared with ruthenium removals of less than 10 percent in otherwise identical argon-atmosphere runs in which no zinc chloride was added to the flux.

Construction of integrated equipment for large-scale ($2\frac{1}{2}$ kg of skull oxide) demonstrations of the skull reclamation process has been started. This equipment will closely simulate plant equipment.

A thixotropically cast beryllia crucible (4-inch OD, 9 inches high) performed satisfactorily in a 184-hour test simulating the conditions encountered in the precipitation and retorting steps of the skull reclamation process. The test was performed on a 180-gram-uranium scale. No significant change in the condition of the crucible was detected after thermal cycling eighteen times between 450°C and 800°C. A metal deposit was noted on the external surface of the crucible at the end of the test, but the amount of deposit was not considered large enough to cause difficulties in full-scale process applications. The metal deposit is attributed to condensation of magnesium-zinc vapor on the external surface of the crucible.

c. Blanket Processing Studies - The sixth of a series of 500-gram-uranium scale blanket process demonstration runs was completed. The blanket process involves dissolution of plutonium-bearing blanket material in a zinc-rich alloy, precipitation of uranium by addition of magnesium, and removal of the supernatant containing the plutonium. Isolation of the plutonium from the supernatant may be accomplished by evaporating the magnesium and zinc. A 90 percent removal of the plutonium-bearing supernatant was achieved in the current run. The plutonium separation factor (from uranium) was 181, and the plutonium material balance was 99.5 percent. The results obtained in this run are in substantial agreement with results obtained in other runs (see ANL-6477, page 47 and Progress Report for June 1962, ANL-6580, page 23).

The phase separation procedure used to effect the separation of the plutonium-bearing supernatant in the blanket process is currently being demonstrated on a full plant scale. The apparatus, which consists of a reactor, a heated transfer tube, and a receiver, is capable of transferring 50-kg-scale batches of liquid metals. In a trial run, 95 percent of a 24-kg charge of 50 weight percent magnesium-zinc alloy at 500°C was transferred into the receiver. In another run, a charge of 4 kg uranium,

25 kg zinc, and 4 kg magnesium was stirred at 790°C for eight hours, after which 20 kg of magnesium was added to precipitate the uranium. After cooling to 420°C, a 93 percent transfer of the zinc-magnesium supernatant was achieved.

d. Plutonium Recovery Process - Distribution coefficients of uranium, plutonium, and praseodymium when present alone between zinc-magnesium solution and molten magnesium chloride at 800°C were reported previously (see Progress Report for April 1962, ANL-6565, page 27). Co-distribution behavior of uranium, plutonium, and praseodymium when present together in the same liquid metal-molten salt media at the same temperature was found to be identical to the behavior of these elements when present alone. The effect of varying temperature on the plutonium-praseodymium separation factor was determined in the same metal-salt system. On decreasing the temperature from 850° to 620°C, the separation factor increased from about 25 to 47.

e. Reduction of Thorium Dioxide - Further results on the reduction of thorium dioxide by zinc-five weight percent magnesium in the presence of a calcium chloride-magnesium chloride-magnesium fluoride flux at 800°C show that complete reduction can be achieved at final thorium loadings at least as high as five weight percent in the metal phase. Under these conditions, the solubility of thorium metal is exceeded and it is precipitated from the liquid metal solution.

f. Fused Salt Study - The phase diagram of the system lithium chloride-magnesium chloride has been completed (see Figure 12). A minimum is observed at 590°C and about 33 mole percent magnesium chloride. The solid phase appears to be a continuous series of solid solutions across the entire composition range. The major differences between the diagram shown and the literature are that the Argonne work shows generally higher liquidus and solidus temperatures and a relocation of the minimum from 40 to about 33 mole percent magnesium chloride.

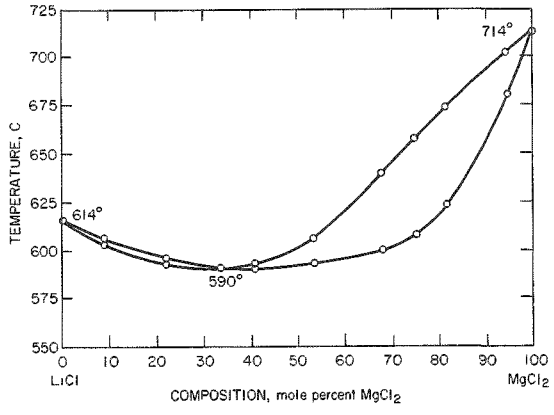

Figure 12. Lithium Chloride-Magnesium Chloride System

g. Materials Evaluation - A pressed-and-sintered tungsten crucible ($5\frac{1}{4}$-inch OD by 12 inches high) appeared to be unaffected in two successive 500-hour runs at 800°C made under conditions of the noble metal extraction step and the skull oxide reduction step of the skull reclamation process. A molybdenum-30 percent tungsten agitator was pitted somewhat after the first 500-hour run, but did

not appear to have undergone additional corrosion in the second 500-hour run. It has been concluded that both tungsten and molybdenum-tungsten alloy are suitable materials of construction for use in the skull reclamation process.

Several cement and aggregate compositions are being evaluated as mixes eventually to be used for making large crucibles by the method of concrete casting. The materials of construction must be resistant to attack by uranium-magnesium-zinc-halide salt systems. Samples have been prepared from fused alumina, magnesia, and beryllia aggregates mixed with cements containing three or four of the following components: CaO, Al_2O_3, MgO, SrO, and BaO. These samples are being tested to determine their resistance to corrosion by process solutions. Experimentation with materials for providing an impervious coating to the interior of the crucible has also begun.

h. Special Projects - Studies were continued of mass transfer in liquid metal systems. Solution-rate coefficients have been determined for the dissolution of small uranium cylinders in agitated cadmium.

The diffusivity of uranium in liquid bismuth was found to range from 2.5×10^{-5} sq cm/sec at 500°C to 4.6×10^{-5} sq cm/sec at 725°C with estimated accuracies of ± 15 percent.

D. FARET

The general engineering and physics parameters of an experimental facility to test the characteristics of advanced fast reactors are being examined in detail.

The safety aspects of the FARET heat removal system are under study. Design features of the following items were studied: (1) a 15-ft high vertical U-tube primary heat exchanger; (2) an emergency pump and associated check valves connected in parallel with the primary pump; and (3) an expansion tank. It was found that the natural thermally-induced circulation rate of coolant was insufficient in the preliminary design. However, by slanting the primary heat exchanger (average placement approximately 3.5 ft above the bottom of the core), the natural circulation rate would be improved to provide a heat removal rate equivalent to 3% of the design power, based upon a 300°F coolant temperature rise through the reactor.

The stress analysis of an improved main coolant pipe configuration for the FARET reactor facility has been completed. The improved design configuration was fitted within the available space of the reactor containment building. The results of the study indicate operating stresses of 75, 95, and 48% of the allowable code stresses at a maximum of 7,000 thermal cycles from room temperature to 1200°F in the reactor-heat exchanger, heat exchanger-primary pump, and primary pump-main reactor coolant pipe section, respectively.

A second scheme is being studied in which two primary pumps in series without check valves are placed in an enlarged expansion tank and are surrounded by a circular-shaped heat exchanger. Such an arrangement would assure sufficient natural circulation to provide adequate shutdown cooling capacity.

III. GENERAL REACTOR TECHNOLOGY

A. Applied Reactor Physics

1. Experimental Van de Graaff Studies

a. The Differential Scattering of Fast Neutrons - The nanosecond pulsing and timing equipment was utilized in neutron scattering measurements from incident energies of 0.3 to 1.5 Mev. The experimental results were expressed in the conventional Legendre form

$$\frac{d\sigma}{d\Omega}(\text{elastic}) = \frac{\sigma_t\,(\text{elastic})}{4\pi}\left[1 + \sum_{i=2}^{5} W_i P_i\right]$$

where W_i's are measured coefficients and P_i's the Legendre polynomials. Figures 12a-f give the results of this research as it pertains to elastic scattering from W^{184}.[1] The solid points in the figures pertain to elastically scattered neutrons only, the spectrometric resolution of the system being sufficient to resolve the elastic and inelastic components. Results, such as those shown for W^{184}, can be used to obtain the transport cross section usually employed in multigroup reactor calculations. An example of the transport cross section so obtained is given in Figure 13. The solid curve represents the transport cross section of U^{238} as derived from measurements by this group.

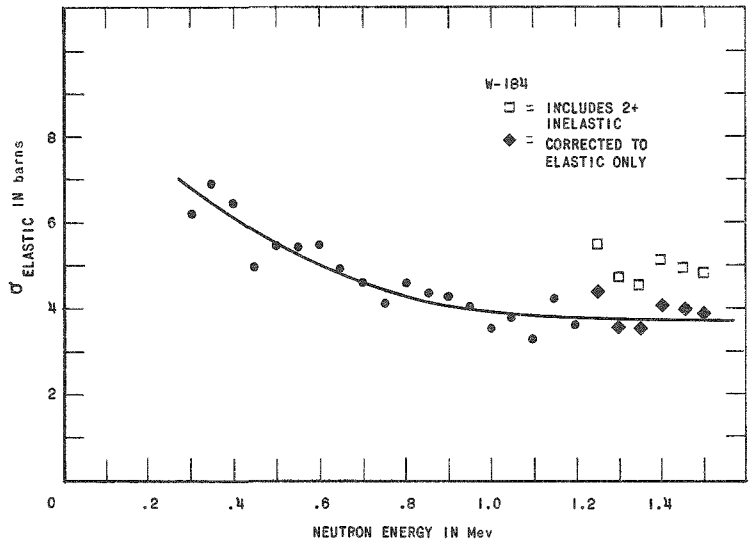

Figure 12a. Total Elastic Scattering Cross Section of W^{184}.

[1] These W^{184} results, in part, fulfill a priority I request for basic nuclear data.

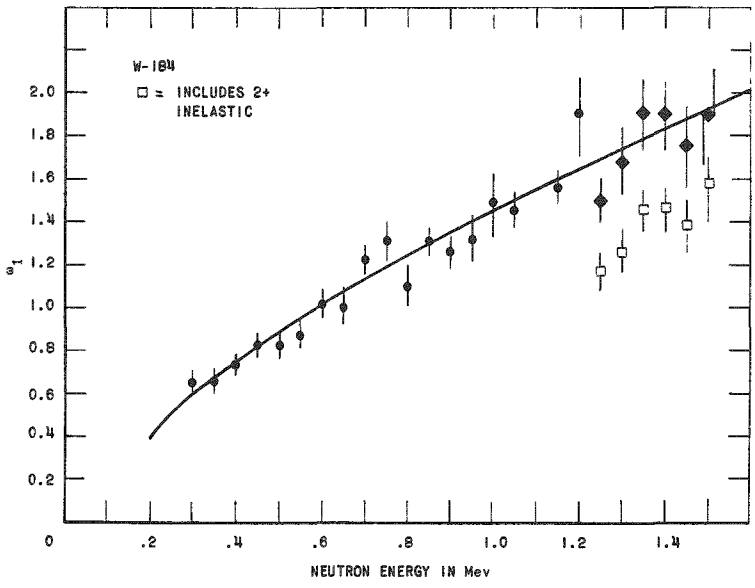

Figure 12b

ω_1 Coefficient of W^{184}

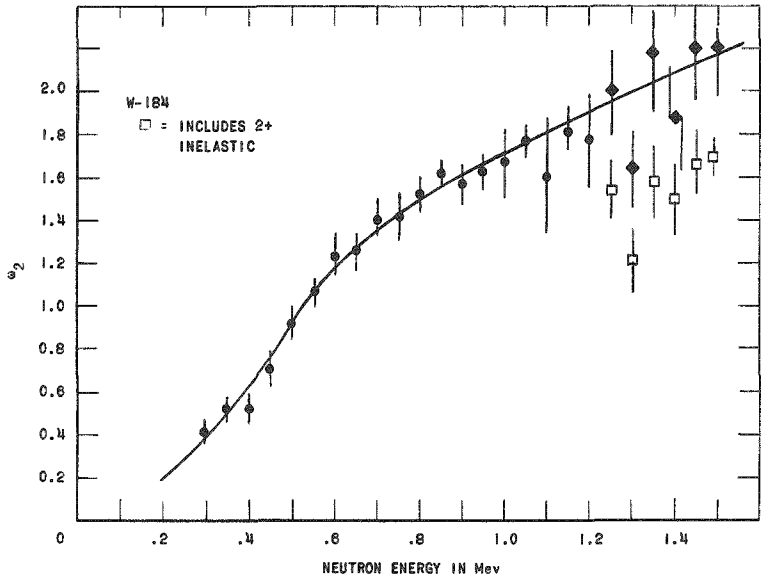

Figure 12c

ω_2 Coefficient of W^{184}

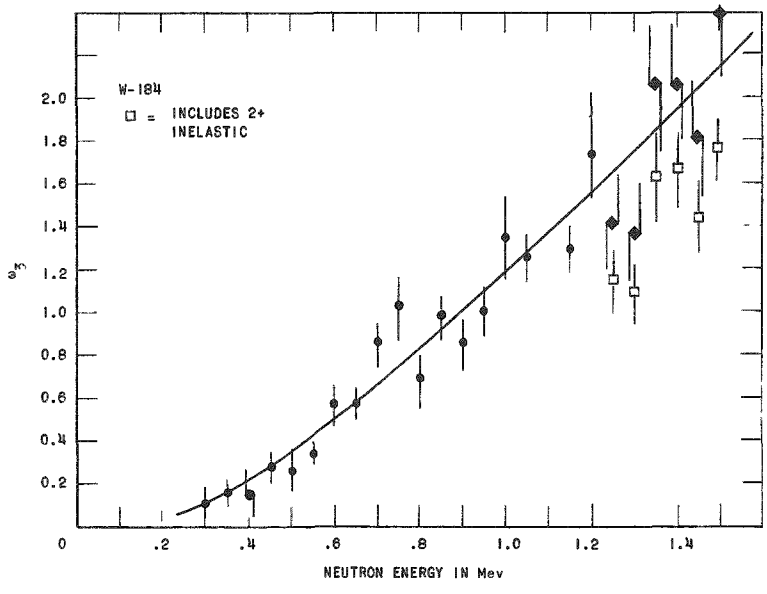

Figure 12d

ω_3 Coefficient of W^{184}

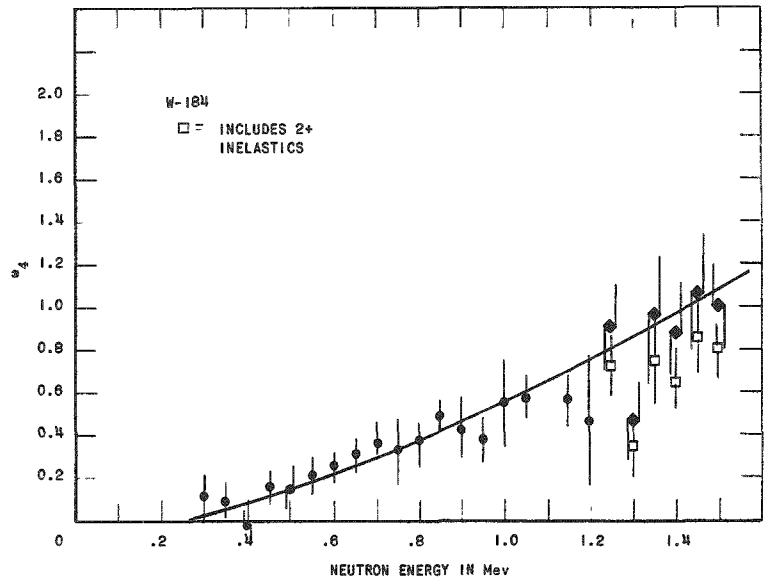

Figure 12e

ω_4 Coefficient of W^{184}

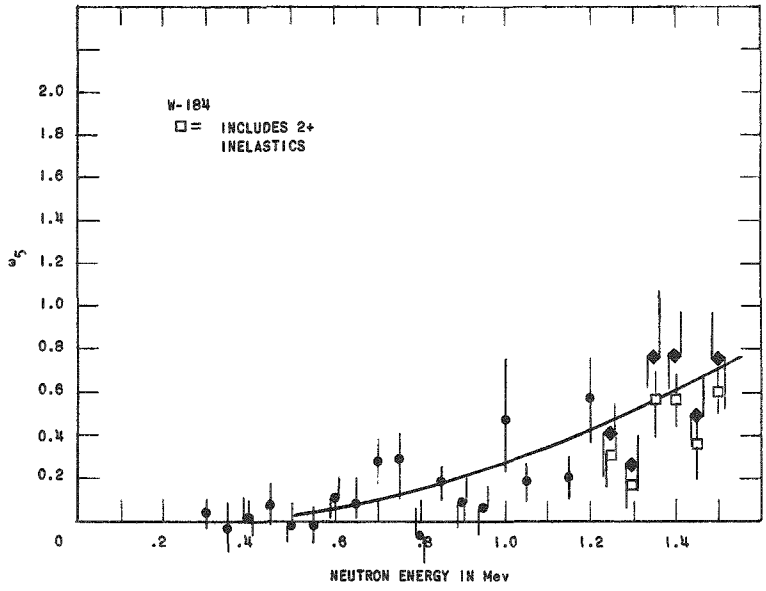

Figure 12f

ω_5 Coefficient of W^{184}

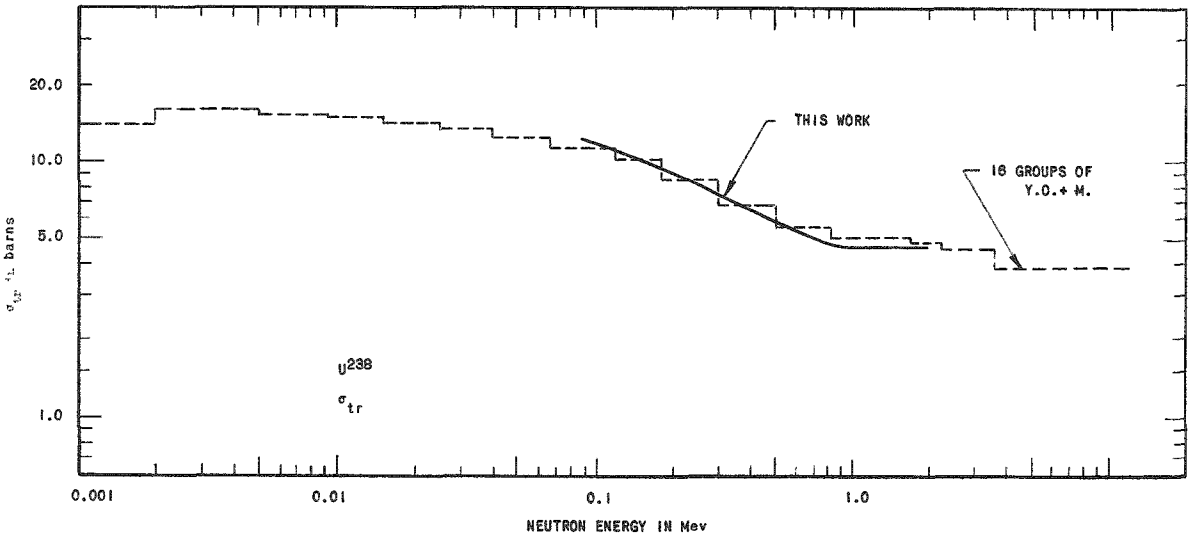

Figure 13. Transport Cross Section of U^{238}

The dotted histogram represents the transport cross section given by a widely used 16-group fast reactor cross section set.[2] It is evident that there exists in the neighborhood of 1.0 Mev a discrepancy of about 10% between the measured transport cross section and that accepted in the multigroup set.

b. Total Neutron Cross Section Measurements for Fe, Ni, and Cu - The n-γ discrimination detector was utilized to measure the total neutron cross section of natural iron, nickel and copper. The measurements were made with about 20 kev neutron energy resolution and covered the range of incident neutron energies from 600 kev to 1500 kev. The results are shown in Figure 14. The n-γ discrimination detector is particularly suited for total cross section measurements above about 600 kev since effects due to the second neutron group from the Li(p,n) source reaction are eliminated.

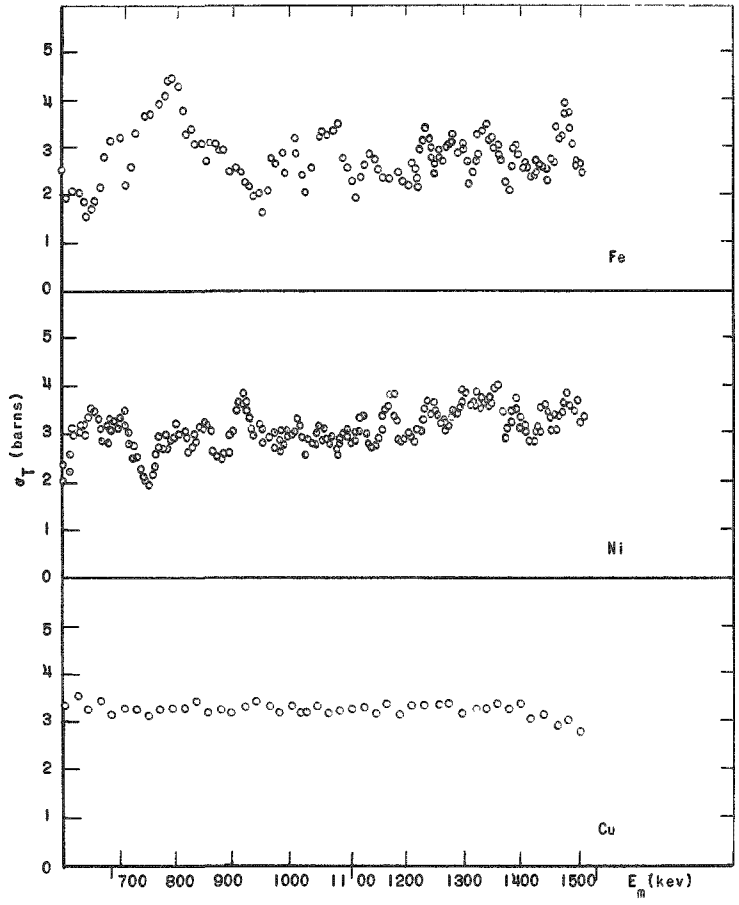

Figure 14. Total Neutron Cross Sections of Fe, Ni, and Cu.

c. Instrumentation - Extensive modifications of the Van de Graaff accelerator were completed. These changes included a complete new high voltage head. One component of this unit was a pulsed radiofrequency ion

[2] "Fast Reactor Cross Sections," Yiftah, Okrent and Moldauer, Pergamon Press, New York, 1960.

source of advanced design. Initial operation has commenced without any major malfunction occurring. The new ion source will permit some new type experiments to be performed with this machine. Among them will be the study of double neutron scattering. Such measurements are expected to contribute to an understanding of the effects of spin-orbit forces in neutron scattering.

2. Theoretical Physics

a. Fuel Cycle Program Development - The version of the CYCLE code which is applicable to the study of the variation of the isotopic concentrations over the equilibrium cycle has been separated and designated as code 1547/RE-282 or CYCLE-2. CYCLE-2 permits the cross sections to be varied over the equilibrium cycle by accepting cross section correction for two fiducial points. In general, four such correction factors are entered for each energy group and for each material which is to vary. CYCLE-2 allows up to four energy groups to be varied. Two of the correction factors refer to maximum and minimum burnup at a minimum value of some regional property, i.e., void fraction, water/metal ratio; and the other two for the maximum and minimum burnups at a maximum value of the regional property. The code then linearly interpolates to get the cross section correction factor for the current value of burnup and regional property concerned. Cross section factors may be applied to capture, transport, and fission cross sections.

The use of a flux tape at the start of a problem for both CYCLE and CYCLE-2 as now coded is optional. Thus, only the program tape 1 and cross-section library tape 5 are required in addition to the input data tape 9.

CYCLE is being programmed to permit the option of defining the burnup to refer either to reactor burnup or total fuel burnup. The latter definition would be useful in the case of the fast-thermal reactor complex for which the fuel supplied to the thermal reactor has already received some burnup in, say, a fast reactor blanket.

b. Reactor Physics Data Analysis - ZPR-VII - A Fortran code is being written which will calculate cadmium (or other material) cutoff values for an isotropic or beam flux in slab geometry. The flux distribution may be either a Maxwellian with a $1/E$ tail or a flux specified at each energy point. Debugging of the various options of the code is nearly complete.

Calculation of the ratio of fissions in U^{238} to total fissions (δ^{28}) and fast fission factors (ϵ) for the BORAX-V and Hi-C lattices using three independent sets of cross sections are in progress. The three sets

of the cross sections are: (1) the set published by Fleishman and Soodak[3] which were previously used in BORAX-V calculations; (2) the set derived from the GAM-I library tape; and (3) the set derived from the MUFT-4 library tape.

B. Reactor Fuels Development

1. Corrosion Studies

a. Aluminum Powder Products - In December 1961 samples of several varieties of powder product tubing made by the Armour Research Foundation were placed in a 290°C refreshed autoclave. Among the tubing types were those prepared from: (1) as atomized alloy A288 (1% Ni, 0.5% Fe, 0.1% Ti); (2) as atomized A341 (1% Ni, 0.5% Fe, 0.3% Cr, 0.2% Zr, 0.1% Ti); (3) A288 powder ball milled 48 hours; (4) A288 powder ball milled 72 hours.

The surviving powder product tube samples were examined after about $7\frac{1}{2}$ months in water at 290°C. There have been great differences in the corrosion behavior of tubing of the same nominal preparation technique. At present only two specimens of the "as atomized" tubing (vacuum heated before corroding) remain in excellent condition from the thirty assorted initial samples. Only three samples from one length of the 48 hour ball milled powder extrusions are in good condition. No samples survive in good condition from either the A341 (stronger) as atomized tubing or the 72 hour ball milled tubing.

Metallographic examination of the as received tubing indicates widespread porosity and numerous chunky inclusions. Metal flow lines are visible in the 48 hour ball milled material in the as polished condition and become very pronounced on etching. The corrosion resistance has been surprisingly good in view of the poor microstructure of these extrusions.

Samples of corrosion resistant aluminum powder product have been obtained from the French workers at Trefimetaux. These extrusions are being rolled to an equivalent metal surface/metal volume ratio as previously tested tubing and will then be corrosion tested under similar conditions.

b. Light Alloy Suitable for Use with Mercury at Elevated Temperatures - Work continues on the development of lightweight and mercury resistant materials for specific nuclear power reactor applications.

---

[3]Morton R. Fleishman and Harry Soodak, "Methods and Cross Sections for Calculating the Fast Effect," Nuclear Sci. and Eng. 7, 217-227 (1960).

As reported in the July 1962 Progress Report, four nitrided titanium alloys showed little weight change in mercury at 538°C. A subsequent metallographic examination of the transverse section of these tested specimens revealed the following:

1) The nitrided layers of Ti-7 wt-% Al-12 wt-% Zr and Ti-3 wt-% Al-5 wt-% Cr are noteworthy for the high degree of attack by mercury vapor although there was no evidence of significant attack by liquid mercury under same testing conditions.

2) The nitrided layer of Ti-8 wt-% Mn alloy is intact in both the liquid and vapor phases of mercury. Recrystallization has resulted in very large grains with fairly heavy white grain boundaries encircling an acicular structure.

3) In the nitrided Ti-2.5 wt-% Al-16 wt-% V alloy, large grains have recrystallized and are well covered with a basketweave structure. There is evidence that the nitrided layer has united with some white particles, presumably Ti-Al-V-N compound of unknown composition, which tend to diffuse into the base metal. In one or two instances, some of the white particles are observed at the grain boundaries but for most part the boundaries are quite heavy, suggesting an accumulation of the white particles in the boundaries and a further phase transformation occurring. The corrosion attack is moderate and is the uniform solution type.

The exact nature of these nitrided layers is not understood at this time. However, metallographic observation indicates that the alloy composition has a definite effect on the mercury resistance of nitrided layers.

2. Ceramic Fuels

a. Uranium Sulfide Compatibility Tests - An effort is being made to evaluate the compatibility of US with many high temperature and fast reactor cladding materials. A satisfactory technique has been worked out in which 25 v/o of metal filings are mixed with US powder, compacted to $\frac{1}{4}$ in. diameter by $\frac{1}{8}$ in. pellets and fired to the desired temperature. Any reactions or lack of them can be detected by a combination of weight change, polished section examination and X-ray diffraction.

Initial runs have been made with Ta and Mo metal filings, firing the mixture at 1830° and 1930°C for two hours in argon. There was no reaction whatsoever between Mo and US up to 1930°C. The weight of the compact remained constant, eliminating the possibility of the formation of volatiles. There was no apparent reaction between the US and the Ta; however, the Ta particles were perhaps 60% converted to a secondary phase tentatively

identified as TaN from X-ray patterns and weight gain. The N would have been scavenged from the argon furnace atmosphere. Duplicate runs will be made in vacuum.

b. Uranium Sulfide-Thorium Sulfide Solid Solutions - A series of US-ThS solid solution bodies are being prepared for property study by two methods: (1) by homogenizing mixtures of the low temperature sulfide powders, and (2) by firing mixtures of the homogenized powders. Method (2) has been used previously and in one hour firings required a temperature of 2000°C for complete solid solution. Visual examination of X-ray films indicates that method (1) has resulted in complete solid solution at temperatures ranging from 1700° - 1800°C in vacuum.

c. Uranium Phosphide Study - The objective of this study is to characterize the various compounds in the U-P binary system and evaluate their potential as reactor fuel materials. Compounds are being made by direct reaction of the elements using methods described in the July Progress Report.

The reaction is highly exothermic. Temperatures in excess of 2000°C are reached within seconds after the reaction is triggered (which occurs between 400° - 450°C). With the exception of oxygen contamination, essentially single-phase UP is formed when U + P are reacted in the above manner. The oxygen contamination is estimated to be about 0.5 wt-% and is thought to come from the uranium powder which is produced by hydriding. Since a small amount of oxygen ties up a relatively large amount of uranium, the quantity of UO_2 present is about 5 wt-%. Efforts will be made to eliminate or reduce the oxygen contamination.

UP is a brittle, metallic-appearing material. It has the NaCl or rock salt-type crystal structure typical of some of the other interstitial uranium compounds, such as UC, UN and US. Preliminary crystallographic data show it to have a lattice constant of 5.57Å, which corresponds to a theoretical density of 10.3 g/cc.

A small sample of UP was melted in the arc-melting furnace. It melted easily and formed into a dense button. X-ray diffraction revealed that negligible oxidation occurred during grinding of UP in air using a mortar and pestle.

3. Irradiation Studies

a. Irradiation of UC-PuC and PuC - Two full size fuel rods fueled with UC-PuC and PuC have been disassembled and examined after irradiation in the EBR-I reactor. One rod contained alternate slugs of fully enriched, arc-melted UC-20 wt-% PuC (nominal) and PuC. The carbon content of the mixture and pure carbide ranged from 4.75 to 5.73 wt-%.

The slugs were predominantly 1 in. long with a nominal diameter of 0.30 in. The second rod contained pressed and sintered pellets of fully enriched UC-20 wt-% PuC. The pellets averaged 55.1% of theoretical density and contained an axial hole to accommodate a central thermocouple. The pellets ranged in length from $\frac{3}{8}$ in. to $\frac{7}{8}$ in. with a nominal 0.31 in. diameter. Bonding between the fuel and stainless steel cladding was provided by a 0.030 in. NaK annulus.

In the rod containing the arc-melted specimens the PuC specimens had an average calculated metal atom burnup of 0.092 a/o (maximum of 0.102 a/o) at a calculated maximum central fuel temperature of 650°C. The UC-20 wt-% PuC specimens had an average calculated metal atom burnup of 0.071 a/o (maximum of 0.079 a/o) at a calculated maximum central temperature of 460°C.

The fracture resistance of the arc-melted UC-PuC specimens was superior to that of the PuC specimens. The UC-PuC specimens were removed from the rod whole or broken into no more than two pieces. Subsequent handling, however, caused these specimens to break up into as many as six pieces. No conclusion could be drawn concerning a relationship between carbon content and fracture resistance in either the UC-PuC or PuC. Density decreases of 0.00 to 1.05% in the UC-PuC showed no correlation with carbon or plutonium content or with burnup. Increases in diameter of up to 0.004 in. on the few measurable UC-PuC specimens showed a positive correlation with carbon and plutonium content, but the wavy surface condition of the cast specimens throws doubt on the reliability of the measured changes.

The arc-melted PuC specimens were very friable. Though one or two specimens were removed from the rod whole or as two or three pieces, all eventually broke up on handling to from 9 to 26 pieces. Density decreases of 0.45 to 0.75% are random within the PuC specimens and are not significantly different from those of the UC-PuC specimens. The surfaces of the PuC specimens were generally brighter than those of the UC-PuC. In general, the condition of the cast carbide specimens was very similar to those in an EBR-I fuel rod containing UC-PuC and PuC which was examined early in 1961.

The rod fueled with pressed and sintered pellets of UC-20 wt-% PuC achieved an average metal atom burnup of 0.081 a/o (maximum 0.090 a/o). The maximum measured central fuel temperature was 380°C. All pellets were removed intact from the rod. Two pellets were later broken on handling but generally the pellets were very durable. Length increases of up to 0.015 in. and diameter increases of up to 0.004 in. were random and were not considered significant. Density measurements were not made because of the extensive open porosity in the pellets.

The fission gas release from the rod containing the arc-melted UC-PuC and PuC specimens was 0.24% of theoretical. The gas release from the UC-PuC pressed and sintered pellets was 12.01% of theoretical. The low density of the sintered pellets is considered the major factor contributing to the difference. The gas release values are based on the theoretical fission product yields for the fast fission of U^{235} and Pu^{239} derived by Burris and Dillon and reported in ANL-5742. Sufficient gas was available from the sintered pellets to obtain a mass spectrometric analysis of the stable xenon and krypton isotopes and Kr^{85}. Composite theoretical xenon and krypton isotopic ratios for the UC-PuC were calculated by considering the fuel composition and the relative fission rates of U^{235} and Pu^{239} and then applying these factors to the individual isotopic ratios for pure U^{235} and pure Pu^{239} fission. The agreement between the composite theoretical and experimental isotopic ratios for xenon was quite good. The krypton ratios, however, did not exhibit the same good agreement. The composite theoretical Xe/Kr ratio is 9.29:1; experimentally it was 5.48:1. It was also found that whereas 11.25% of the xenon was released, 19.09% of the krypton was released, giving the overall value of 12.01%. It is possible that either krypton is diffusing more rapidly than xenon or the theoretical yield of krypton used in the calculation is low.

In addition, a single vibratory-compacted specimen of PuC with 0.009 in. type 304 stainless steel cladding is being irradiated in different positions of the CP-5 reactor. The fuel was compacted to about 80% of theoretical density in a 2 in. length and 0.156 in. diameter. The carbide contained 6.22 wt-% carbon. The object of the experiment is to obtain information on the heat generation rate of PuC in the part thermal, part resonance flux of different positions in the reactor. Future experiments on plutonium-bearing fuels will be positioned in CP-5 to obtain desired heat generation rates and cladding surface temperatures based on the information gathered in this experiment. To date the specimen has achieved a maximum cladding surface temperature of 435°C at a heat output of 955 watts/in.

b. Postirradiation Examination of Blistered Area in a CP-5 Fuel Element - In the Progress Report, July 1962, ANL-6597, the CP-5 tubular fuel elements were reported to have an Al-U-Ni alloy core clad with X8001 aluminum alloy. Although there are several fuel tubes in the reactor of this composition, the reference fuel element is made up of a binary aluminum-uranium alloy clad with Type 1100 aluminum.

4. Properties of the Thorium - Uranium - Plutonium Systems

Density measurements (see Table IV) were made on thorium-plutonium alloys by the same procedure used for the thorium-uranium alloys reported last month. Measurements were made on as-cast alloys

prepared from crystal bar thorium and high purity plutonium by arc melting. The two-phase region of the thorium-plutonium alloys show the same linear relationship of specific volume versus composition in weight percent as the thorium-uranium alloys. The density of 14.0 g/cm^3 or the specific volume of 0.0714 cm^3/g determined by Poole, Williamson and Marples for the cast alloy $Th_{13}Pu_6$ fits well into this linear relationship (Fig. 15). Unexpectedly, the linear relationship of specific volume versus composition also holds for the region of solid solubility of plutonium in thorium. The intersection of the two lines at 33.6% plutonium indicates that this quantity is the limit of solid solubility in this alloy series.

Table IV. Densities of Arc Melted High Purity Thorium-Plutonium Alloys

No.	Alloy (nominal w/o) Th	Alloy (nominal w/o) Pu	Density at 25°C (g/cm^3)
B772	100	0	11.715
B766	90	10	11.914
B767	80	20	12.131
B768	70	30	12.371
B769	60	40	12.744
B770	50	50	13.139
B773	40	60	13.665

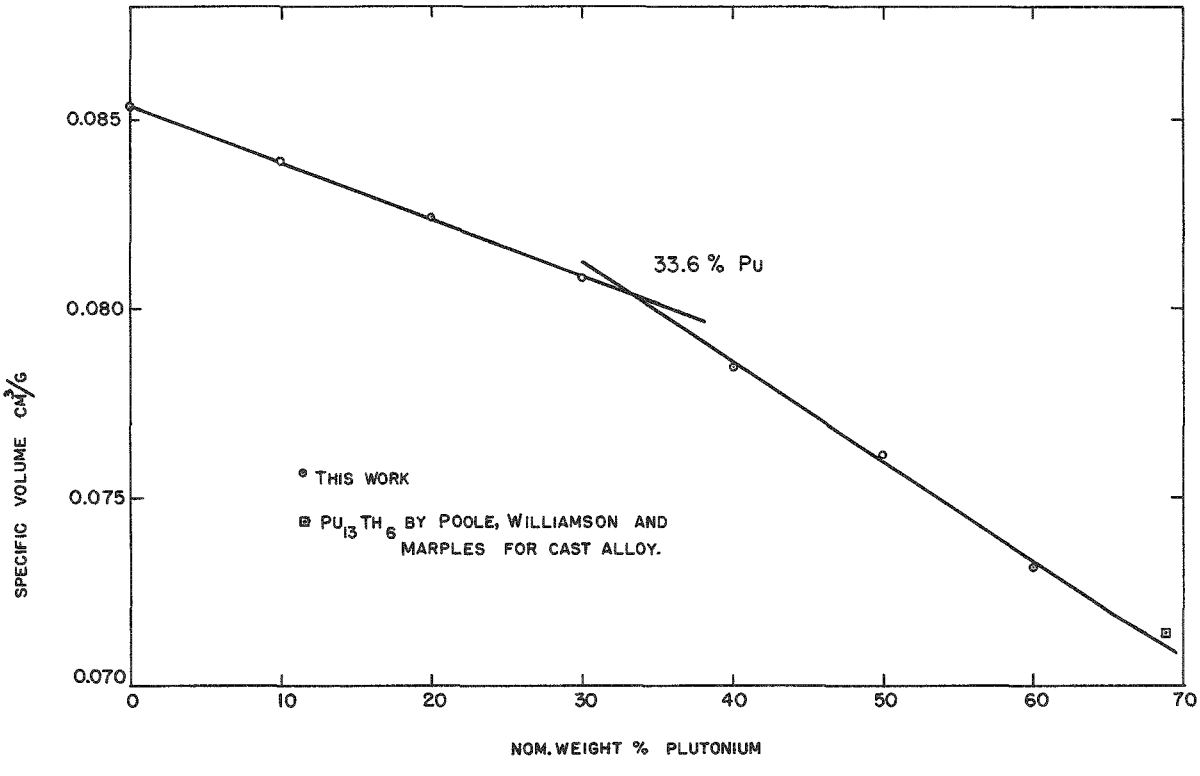

Figure 15. Specific Volume of Arc Melted High Purity Thorium - Plutonium Alloys

Macrometallography of arc melted thorium-uranium alloys distinctly showed the severe segregation that occurs in those alloys which, according to the phase diagram, consist of two liquid phases when molten. This occurred in all alloys of 30% uranium or more with increasing severity as the uranium content increased. While it is usually possible to obtain a quasi-homogeneous distribution of the two phases by melting at a temperature above the stability of the two phase field and cooling rapidly through its temperature range, these conditions apparently have not been met by arc melting. The existence of the two phase field will cause considerable difficulty in preparing uniform alloys in this composition range unless the miscibility gap can be closed by suitable alloy additions.

5. Nondestructive Testing

a. Ultrasonic Techniques

Ultrasonic techniques are useful for measuring material properties and for the nondestructive evaluation of nuclear reactor materials. The ultrasonic techniques program at ANL includes: measuring the elastic constants of single crystals of uranium and zirconium, Lamb and surface wave propagation in flat plates and tubes, ultrasonic attenuation of engineering materials at elevated temperatures, the evaluation of nuclear reactor components such as tubing, and the development of ultrasonic imaging methods.

(1) A Study of the β to α Phase Transformation in Plutonium Using Ultrasonics - Two separate series of measurements of transit time and pulse amplitude versus temperature have been made using the plutonium specimen mentioned in last month's report, and the apparatus discussed in that report. The specimen, mounted in the sound transceiving jig, is slowly raised in temperature (about 0.2 to 0.4°C/min), while the sound is passed through it. From these measurements, plus knowledge of the specimen length and thermal expansion characteristics of Pu, it is possible to calculate the sound velocity and attenuation in the sample as a function of temperature. The temperature range from room temperature to 320°C has been covered; this includes the transformation from the alpha phase, through the beta and gamma phases, and into the delta phase.

The alpha to beta phase change is very striking when plotted on a graph of transit time versus temperature. The transit time changes abruptly by about 35%. The other phase changes are also visible, but are not as striking as the alpha to beta change.

The plots of transit time and temperature between the two runs are quite reproducible. It has not yet been possible to make a cooling run because of technical difficulties at high temperatures. These difficulties are being corrected.

The equilibrium measurements will be useful for comparison purposes when the quenching runs are made. Such measurements have never been made before on plutonium of as high a purity as the specimen being used in these experiments.

(2) Correlation of Heat Transfer Properties and Bond Quality - With the completion of an amplifier (Monthly Report, April, 1962) to be used in conjunction with the reflectoscope and monitor, it has been possible to use this system to provide an output to Alfax recording paper which is proportional to the signal voltage. The complete scanning and recording system has not yet operated satisfactorily, and a complete set of Alfax recordings on the specimens is still to be made.

The charts that have been made of the brazed specimens were made on the basis of a "go-no-go" type output to the recording paper. These charts have shown the bad braze areas, but they have a limited usefulness because they give no indication of the various levels of sound transmission through the braze. These charts have shown large uniform areas of "no transmission" perpendicular to the braze plane in all specimens. However, since these regions were found in the solid copper block they may be due to grain structure. Additional tests will have to be made to separate the effects of larger grain size from bad bonds.

(3) Ultrasonic Imaging Studies - Further studies have been made on the characteristics of the photographic paper in developer method for imaging ultrasonic beams. Although this method is faster in response than the photographic film methods previously studied, the threshold sensitivity appears to be about the same (of the order of 0.5 watts/cm^2). Some images of metal objects have been obtained by these two methods but the image quality is limited by the relatively poor sensitivity of these detectors.

By comparison, some sensitivity measurements on electronically scanned pickup tubes have shown that the tubes respond to ultrasonic intensities of the order of 10^{-7} watts/cm^2. This appears to be the threshold sensitivity of such tubes using either quartz or $BaTiO_3$ piezoelectric faceplates.

Published data on threshold sensitivities of similar tubes have indicated theoretical values of the order of 10^{-9} watts/cm^2. Such values were based on a usable signal-to-noise ratio with the noise signal limited by that generated in the load impedance of the input circuit. The use of a high gain electron multiplier in the pickup tube should change the limiting noise value to that in the scanning beam itself and therefore improve the ultimate sensitivity of the system. This is not the case. The multiplier does improve the signal level so that there is less shielding difficulty but it does not appear to improve the threshold sensitivity of the

system. The limitation on this value now appears to be the piezoelectric voltage variation which can be detected by the scanning beam. Further studies of this development are now in progress.

b. Neutron Imaging

Further studies of the neutron beam facility at the Juggernaut reactor indicate that the cadmium ratio of the emergent neutron beam is approximately 4:1. The presence of this rather high intensity epicadmium component of the beam has introduced some small changes in the relative speeds of several of the metal screen techniques. Speed increases have been noted for rhodium, silver and indium direct exposure techniques, in particular, because of the response of these materials to resonance energy neutrons. Transfer response of these three materials, and that of gold, has also been improved.

The resolution qualities of the neutron beam facility at Juggernaut reactor have also been investigated. Using a cadmium test object containing holes whose spacing continually decreases, the resolution properties of the beam have been obtained by determining how many holes could be resolved on neutron radiographs taken under various conditions. With the test object directly on the cassette, a spacing in the order of 0.001 in. could be resolved. By the time the test object was moved 1 in. away from the cassette however, the divergence of the neutron beam yielded a resolution only in the order of 0.020 in. By comparison, the well defined neutron beam available at CP-5 reactor yielded a resolution value of about 0.005 in. when the test object was 4 in. away from the cassette. The divergence of the beam at Juggernaut, therefore, would make it difficult to inspect thick materials.

A Soller slit, which will remove diverging radiation from the beam and thereby improve the resolution qualities of the beam, is being constructed. Material for this collimating slit is now on order.

c. Resolution Studies in Scintillation Spectrometry

The vacuum chamber and solid state detector system for studying the alpha spectra from plutonium and uranium was put into operation. Primary effort was to determine the resolution possible with this equipment and with source samples prepared by elementary and simplified techniques. To date, it has been possible to resolve the 4.76 Mev alpha particles from U^{234} and the 4.20 Mev alpha particles from U^{238} in normal and low enriched uranium. Resolutions of the order 50 kev were observed for a better quality plutonium source sample. For fully enriched uranium samples prepared by unrefined preparation techniques resolutions of the order of 150 kev were possible.

d. Eddy Current Techniques - Development of the Pulsed-Field Reflection System - This system is being used to test a wide variety of thin-walled tubing as a part of the development effort on the system itself. All of this tubing is subjected to routine eddy current testing on the dual frequency test system, but sample quantities are then tested using the pulsed equipment. The pulsed system has in a majority of these tests shown superior signal-to-noise ratio over the older test system, especially in tubing with wall thicknesses less than 0.020 in. The optimum frequency or pulse length is chosen in each case, and then the two systems are compared using the same defective tubes and identical rotational and translational speeds. A $\frac{1}{16}$ in. aperture has been used on the mask-aperture assemblies of the pulsed-field reflection system, but the tests on tubing of less than 0.020 in. wall indicate that an aperture of 0.045 in. might provide a worthwhile increase in resolution. A new mask aperture assembly with a 0.045 in. aperture is being constructed to check this possibility.

It has been found that occasional lots of thin wall tubing are encountered in which narrow zones of cold worked material are found near the inner surface or outer surface, or both. A transverse cross section of this material will show this zone as narrow strata of material with an appreciably finer grain structure than the rest of the tube. This condition was easily detectable by eddy current test equipment, which is at first surprising since variations in grain size are of minor importance in most eddy current test problems. It has since been deduced that the effect of the cold worked material on the output signal is due to the presence of a second phase which possesses appreciable permeability. It is easily eliminated by either a complete anneal or a d.c. field strong enough to saturate the small amount of this second phase present. The pulsed-field reflection system is appreciably less sensitive to this condition than the sinusoidal systems due to the stronger field around the aperture which accomplishes some of the saturation itself.

C. Reactor Materials Development

1. Radiation Damage in Metals

a. Magnetic and Dynamic Properties of SA-212B Steel - The a-c and d-c- magnetic properties of SA-212B carbon steel were measured before and after irradiation in the EBR-I. The steel is ASTM reference material in the form of multinotch impact bars. The irradiations ranged from 2 to 60 Mw-hr in the EBR-I core (see June Monthly Report, ANL-6580, p. 39). No change could be detected in the d-c coercive force, measured after magnetization at 1300 oersteds. Photographs of families of 60 cps hysteresis loops showed no detectable change in magnetic permeability, remanence, a-c coercive force, magnetization, or core losses.

Similar samples of material were irradiated in CP-5 and MTR. The CP-5 irradiations showed a 250°F NDT shift (March Monthly Report, ANL-6544, p. 42) and the MTR irradiations showed appreciable changes in hardness and impact properties. These samples also failed to show significant changes in magnetic properties.

Heat treatment and mechanical working which introduce stresses as well as extensive mechanical property changes are often accompanied by changes in the magnetic properties discussed above. The magnetic measurements made to date were done on irradiated but unworked and unstressed material (SA-212B) and did not reflect comparable mechanical changes. The next series of measurements contemplated will be made on irradiated materials having had previous stress histories.

The studies of the sonic properties of irradiated steel are continuing (January Monthly Report, ANL-6509). A new suspension stand was constructed which utilizes micro-positioners for the placement of acoustic bars on the suspension wires for the measurement of resonant and harmonic frequencies (transverse vibration mode). The design includes dead-weighted lever arms to maintain a constant tension on the suspension wires and thus eliminate the damping influences of the wires over the temperature range of interest (between room temperature and 180°F). Reproducibility of measurement was greatly improved; all sonic properties of SA-212B were remeasured and the bars were encapsulated for irradiation in the EBWR.

b. Quenched and Tempered 2-$\frac{1}{4}$% Chromium-1% Molybdenum Pressure Vessel Steel - Multinotch impact bars of quenched and tempered 2-$\frac{1}{4}$% chromium-1% molybdenum steel, originally considered for the ARBOR pressure vessel, were encapsulated for irradiation in EBR-I. The plate was water-dip quenched to produce a homogeneous martensitic structure and tempered at 1100°-1150°F to produce an impact resistant steel (15 ft-lb at -50°F). The material as well as its analysis and history was obtained from the Babcock and Wilcox Company.

c. SL-1 Pressure Vessel Steel - A number of mildly radioactive sections of the upper portion of the SL-1 pressure vessel have been received for examination of radiation effects in the stressed SA-212B steel.

Examinations contemplated include, in addition to the standard measurements, the following: (1) radiography of welds; (2) bond strength; (3) crack propagation resistance; and (4) strain hardening effects.

The as-built radiographs were obtained from the vessel fabricator (Lasker Boiler and Engineering Corporation). A summary of the operating history of the SL-1 was obtained for estimating the integrated exposure received by the vessel.

d. Encapsulation Procedures for EBWR Dosimetry - Irradiation capsules used to house the dosimetry foils are now subjected to a 30 to 60-minute evacuation procedure prior to filling with helium to eliminate corrosion problems (ANL-6509, p. 37). Two dosimeter and five surveillance capsules were placed in the EBWR and irradiated at power levels up to 40 Mw. One dosimeter and one "bare" location surveillance capsule (containing SA-212B multi-notch impact and combination magnetic-acoustic bars) have been thus far removed from the EBWR reactor for examination.

e. Irradiations of Steel in EBR-I - Multinotch Izod specimens of SA-212B carbon steel, described in (a) above have been broken in high-level caves. A preliminary analysis of the results gives a dependency of the ductile-brittle transition temperature shift between $(\phi t)^{1/3}$ and $(\phi t)^{1/2}$, where ϕt is the integrated neutron exposure. Since some data showed considerable scatter, several duplicate irradiations were performed.

f. Dosimetry in EBR-I - A set of $Al_2(SO_4)_3$ packets was irradiated in EBR-I. These will furnish activation rates for the reaction $S^{32}(n,p)P^{32}$, which will permit an absolute normalization of flux spectra and damage rate calculations. Similar irradiations are being carried out in CP-5 and these will be used for comparison of spectral calculation between the two reactors.

Nickel monitor wires which were included with the EBR-I steel irradiations were counted both before and after radiochemical separation of the Co^{58} formed in the $Ni^{58}(n,p)Co^{58}$ reaction. Preliminary comparisons reveal an apparent loss of about 8% of the activity in most of the radiochemical separations, although a few results appear to be more seriously out of line. Since EBR-I has no thermal neutrons, the Co^{58} peak can easily be counted without correcting for competing peaks. However, if a similar technique is used for foils irradiated in a thermal reactor, other activities, particularly Co^{60}, complicate the gamma ray spectrum and appropriate corrections have to be made.

The reaction $Fe^{54}(n,p)Mn^{54}$ ($T^{1/2}$ ~300 d) offers a valuable monitor for iron irradiations. For EBR-I work this peak may be counted directly; however, in preparation for its use in CP-5 and other thermal reactors, in which competing activities are produced, a radiochemical separation is being evaluated. A systematic loss of activity is also observed in this process and changes are being made in the technique to make it more quantitative.

Based on existing cross section data for S^{32} and Ni^{58} agreement between calculated and measured fluxes appears very encouraging. The Fe^{54} cross section is not known, but at least the relative activations as a function of exposure time coincide with predictions.

D. Chemical Separations

1. Fluidization and Volatility Separations Processes

a. Direct Fluorination of Uranium Dioxide Fuel - Laboratory work has continued on the development of a method for the removal of plutonium by fluorination from mixtures of uranium dioxide, plutonium dioxide, oxides of fission product elements, and alumina. A new processing scheme (see Progress Report, July 1962, ANL-6597, page 41) is being investigated. In this scheme, the uranium dioxide pellets are oxidized prior to fluorination in order to convert the material into a uniform, fine powder of U_3O_8. The use of this powder in the fluorination step makes the complete fluorination of the plutonium to the hexafluoride easier to carry out.

In the current experiments, solid solutions of uranium dioxide and plutonium dioxide containing oxides of fission product elements, in the form of pellets and also in the form of powder, were reacted for three hours at 450°C with 20 percent oxygen in nitrogen. The product of the oxidation (a fine, black powder) was mixed with Alundum and then reacted with fluorine. The plutonium dioxide-uranium dioxide solid solution contained about 0.3 wt-% plutonium and about one percent of a mixture of 10 fission product element oxides (BaO, ZrO_2, La_2O_3, CeO_2, Y_2O_3, Nd_2O_3, Sm_2O_3, Pr_6O_{11}, Eu_2O_3, and Gd_2O_3). After the mixture had been oxidized, fluorinations were carried out in two 10-hour steps, one at 450°C with a mixture of 10 percent fluorine, 25 percent oxygen, and 65 percent nitrogen, and the other at 550°C with a mixture of 75 percent fluorine and 25 percent oxygen. In seven experiments, these fluorinations resulted in the removal of about 99.4 percent of the plutonium in the original mixture. This is equivalent to a retention of plutonium in the inert solid of about 0.006 wt-%. This is the lowest retention of plutonium obtained to date.

In one of these experiments, the Alundum used had been previously employed as an inert bed in the chlorination of stainless steel, and contained the chlorides of iron, nickel, and chromium. The presence of these materials in the Alundum did not hinder the removal of plutonium from the mixture.

In recent pilot plant-scale studies, two batch fluorination runs were made at 500°C with 12-in.-deep uranium dioxide pellet beds for preliminary evaluation of a two-zone oxidation-fluorination scheme for the production of uranium hexafluoride. The two zones consist of a relatively deep fluidized bed of alumina with a portion of the lower part of the bed occupied by a static bed of uranium dioxide pellets. An oxygen-nitrogen mixture is introduced as fluidizing gas at the bottom of the reactor and fluorine gas is introduced at the top of the uranium dioxide pellet bed.

Oxide fines (U_3O_8) are elutriated from the pellet bed and carried to the upper zone where they are fluorinated in the fluid bed of alumina. In the first run, the fluidizing gas rate was 1.3 ft/sec. In the lower zone, the oxygen concentration (in nitrogen) of the inlet gas was varied from 3 to 8 percent; in the upper zone, the fluorine concentration in the fluorinating gas was varied from 5 to 13 percent (oxygen 3 to 6 percent, balance nitrogen). Although performance varied during the batch operation, it was found that, in the latter portion of the run, uranium hexafluoride collection rates were as high as 70 lb UF_6 per hour per sq ft reactor cross section, with a fluorine efficiency of over 90 percent. This run was satisfactory except for heavy fines deposits in the upper (disengaging) section of the reactor. These fines were removed by a separate fluorination at about 200°C.

In the second run made at a fluidizing gas rate of 0.9 ft/sec, an oxygen concentration of 4 percent and a fluorine concentration of about 12 percent (balance nitrogen), lower production rates, which averaged 30 lb UF_6 per hour per sq ft reactor cross section and lower fluorine efficiencies, which averaged 53.6 percent, were obtained, probably because of fines accumulation in the uranium dioxide pellet zone. To obtain a better elutriation of the fines from the pellets, somewhat higher gas rates are deemed necessary. Further tests are planned with the two-zone system under conditions designed to obtain control of fines formation by independent temperature regulation of the lower zone.

Fluidization studies related to the direct fluorination process are being made. In four preparations of uranium oxide fines from pellets oxidized at 500°C, complete freedom from caking was found only in a run with a 4-in. pellet bed in a 16-in. alumina fluid bed, which was fluidized with 10 percent oxygen in nitrogen at a gas rate of 1.5 ft/sec. Beds of 13-, 24-, and 59-in. uranium dioxide pellet depth showed that caking tendencies increased with pellet bed depth.

Rates of mixing of fine (120 to 200 mesh) solids fluidized in the voids of packing that simulates uranium dioxide pellets of various sizes are being measured. Pseudo-diffusion coefficients show a regular increase with fluidizing gas rate in tests to date. Coefficients increased from 0.35×10^{-3} to 2.4×10^{-3} sq ft/sec for gas rates of 0.3 to 1.5 ft/sec, respectively. Agreement of coefficients within a factor of two was obtained for the following packing: $\frac{1}{4}$-in. spheres, $\frac{1}{2}$-in. spheres, and $\frac{1}{2}$-in. cylinders.

Effective thermal conductivities in the axial (longitudinal) direction are being measured on a fluidized-packed bed system. Effective thermal conductivity increases, as expected, with gas flow. Preliminary values of up to about 140 Btu/(hr)(sq ft)(°F/ft) were obtained.

b. Separation of Uranium from Zirconium Alloy Fuels

(1) Studies of the Chlorination and Fluorination Steps with Down-Flow Fixed-Bed Filters - Studies continued on the development of a

fluid bed-volatility process for the recovery of uranium from highly enriched uranium-Zircaloy alloy fuels. The work is being conducted in a $1-\frac{1}{2}$-in. diameter reactor with the alloy submerged in an inert bed (currently Norton Company's Alundum). The scheme involves chlorination of the alloy to remove the zirconium as the volatile tetrachloride followed by fluorination to recover the uranium as the hexafluoride. In current studies, the reaction cycle was modified to include the use of a mixture of phosgene and hydrogen chloride as the chlorinating agent in the initial process step. This step was then followed by a treatment with phosgene alone. This in turn, was followed by the fluorination step. The current studies also included a comparison of the overall uranium retention by two types of Alundum, Type RR and Type 38. Results based on uranium retention show that the overall cycle time, and, therefore, the consumption of reactants are reduced considerably when a mixture of phosgene and hydrogen chloride is used as the initial reactant as compared with the use of hydrogen chloride alone as the initial reactant. In a run in which the following steps were carried out: (1) chlorination with a 4:1 mixture of hydrogen chloride and phosgene, (2) treatment with phosgene alone, and (3) reaction with fluorine, a residual uranium content of 0.04 wt-% in the fluid bed was obtained after an overall cycle time of 9.7 hours. This may be compared with a run in which hydrogen chloride alone was used in the first step. In this run, a residual uranium content of 0.05 wt-% was achieved after an overall cycle time of 19.2 hours. These residual uranium values (0.04 and 0.05 wt-%) correspond to about one percent of the initial uranium charge (5.1 wt-% uranium-Zircaloy alloy chips). At 400°C, the two types of Alundum, Type RR and Type 38, retained about the same quantities of uranium (0.04 and 0.03 wt-% uranium, respectively, of the final beds). However, refluorination of the beds at 500°C achieved very little further removal of uranium in the case of Type 38 Alundum (the residual uranium decreased to 0.02 wt-% uranium from 0.03 wt-% uranium) whereas with Type RR material, the uranium content was reduced to <0.01 wt-% uranium from 0.04 wt-% uranium. Type 38 Alundum appears to have another disadvantage inasmuch as caking of the filter bed occurred during the run in which this type of Alundum was used and which thereby caused an excessive pressure drop in the system.

(2) Fluid-Bed Hydrolysis of Zirconium Tetrachloride - Hydrolysis studies on the fluid bed conversion of zirconium tetrachloride to zirconium dioxide are continuing in an effort to evaluate the effects of operating variables on the extent of deposition (conversion) of the dioxide on the inert bed material (Alundum). Using the quantity of fines found in the bed and on the filters as a basis for evaluating the runs, current experiments made at 350°C in the 6-in. diameter reactor indicated that higher feed rates (in the range 1.8 to 3.3 kg/hr feed) coupled with lower steam excesses (in the range 2.8 to 5.3 times stoichiometric) resulted in increased amounts of fines. The quantity of fines ranged from about 7 to 16 percent in runs of 3- to 6-hour duration.

(3) Pilot Plant for Processing Enriched Uranium-Zircaloy Alloy Fuels - Major items for the pilot plant designed to demonstrate the uranium-Zircaloy alloy fuel reprocessing scheme have been received. These include the primary reactor and hydrolysis column, special high-temperature valves, and the control panel complete with instruments. Installation is expected to be completed by the end of the year.

2. Chemical Metallurgical Process Studies

a. Chemistry of Liquid Metals - Thermal analysis of eight wt-% technetium-zinc alloys indicated a peritectic transformation at about 540°C and the liquidus temperature at about 953°C. The existence of at least two solid intermetallic phases in the system is indicated. This is in agreement with the results of preliminary experiments (see Progress Report, June 1962, ANL-6580, page 45). Work is proceeding on the isolation and characterization of the intermetallic compounds.

Data have been obtained by means of chemical and thermal analysis of uranium-zinc samples which indicate that the transformation of the epsilon phase to the delta phase in the uranium-zinc system occurs at about 790°C. The liquidus temperatures of uranium-zinc alloys containing about 3.8 to 10.5 wt-% uranium ranged from 768° to 862°C (see Figure 16). The break in the curve at about 790°C corresponds to the peritectic, which now appears to be well established.

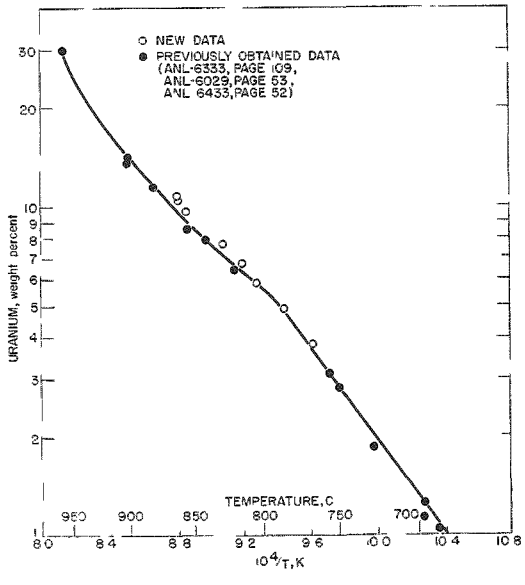

Figure 16. The Zinc-Rich Liquidus in the Zinc-Uranium System

The ternary solid phase found in the uranium-zinc-magnesium system (see Progress Report, July 1962, ANL-6597, page 45) has been isolated in sufficient purity to obtain the approximate composition: 23 wt-% uranium, 64 wt-% zinc, and 10 wt-% magnesium. This corresponds to the approximate empirical formula $UZn_{10}Mg_4$. X-ray diffraction studies indicate that this phase has hexagonal symmetry with a $a = 14.58$ Å and $c = 8.68$ Å.

The solubilities of uranium in a nominal 36 wt-% magnesium-zinc solution were found to range from 1.46 wt-% at 800°C to 0.62 wt-% at 500°C.

Emf data for the galvanic cell, $Pu/PuCl_3$, KCl-LiCl/Pu-Zn (two-phase alloy), have been obtained over the temperature range from 440° to 690°C. The emf over this range may be represented by the equation

$$E \text{ (volts)} = 0.7622 - 7.055 \times 10^{-5} T - 4.361 \times 10^{-7} T^2$$

Preliminary measurements of the magnetic susceptibility of the $ThCd_{11}$ intermetallic compound were made at room temperature and 77.2°K. A small temperature-independent paramagnetism was found. No unpaired spins appear to exist in the system. The preliminary value for the susceptibility of $ThCd_{11}$ was found to be 0.4×10^{-6} emu/g. After correcting for the diamagnetism of cadmium in the alloy, the value for the susceptibility of thorium in $ThCd_{11}$ was found to be 0.54×10^{-6} emu/g. This may be compared with the reported value of 0.42×10^{-6} emu/g for thorium metal at room temperature.

Measurements of the neodymium-cadmium system by means of the recording effusion balance revealed the existence of the following intermediate phases: $NdCd_{11}$, $NdCd_6$, $NdCd_4$, $NdCd_3$, and $NdCd_2$. Two major improvements which were incorporated into the apparatus used for the neodymium-cadmium runs were (1) the use of new effusion cells with small orifice areas which considerably reduced surface depletion effects and thereby led to a better definition of the compounds formed and (2) the adaptation of the recorder to allow a wide selection of chart speeds during a run. This technique, which permits a complete effusion isotherm to be obtained in a single run and which thereby improves accuracy, was used in preliminary reruns of the cerium-cadmium and praseodymium-cadmium systems. Earlier studies of these two systems (see Progress Report, January 1962, ANL-6509, page 43 and Progress Report, November 1961, ANL-6473, page 60) indicated the existence of Ce_2Cd_9 and $PrCd_{3.1-4.2}$ phases, whereas the current investigation indicates that these compounds are $CeCd_4$ and $PrCd_4$.

b. Liquid Metal Distillation - Preliminary experiments are being conducted to determine the extent of entrainment of liquid cadmium in cadmium vapor in the large cadmium distillation unit (see Progress Report, May 1961, ANL-6374, page 27). In these experiments, tin is used as a nonvolatile solute. The concentration of the tin in the cadmium was one percent. The amount of tin carried over to the distillate receiver (presumably by liquid cadmium droplets) is used to calculate the amount of liquid cadmium entrained in the cadmium vapor. The results obtained from five distillation runs indicate that the extent of entrainment is about one percent for cadmium evaporation rates of about 25 kg/hr to 86.5 kg/hr. No clear-cut relationship between liquid cadmium entrainment and evaporation rate was observed.

The nature and magnitude of the boiling and entrainment phenomena of liquid metals is being studied. A fast-response liquid-metal thermocouple system is being developed to follow rapid temperature fluctuations in boiling liquid metals. Surprisingly large, random temperature fluctuations (nearly 50°C) have been observed by means of a cathode ray

oscilloscope during surface vaporization (nonturbulent vaporization) of mercury.

c. Calorimetry - A technique has been developed for the combustion of zirconium diboride in fluorine in preparation for determining the heat of formation of zirconium diboride. Work is now directed toward the development of an analytical technique for determining the amount of unreacted zirconium diboride in the products of combustion.

A second series of combustions of magnesium in fluorine has been performed, thereby completing the combustions. A value of -264.4 ± 0.6 kcal/mole was obtained for the standard heat of formation of MgF_2(c). This differs little from the preliminary value of -265.38 ± 0.70 (see Progress Report, April 1962, ANL-6565, page 46).

The standard heat of formation of CdF_2(c), for which the preliminary value of -167.20 ± 0.20 kcal/mole was presented in Progress Report for April 1962, ANL-6565, page 46, was recalculated using more accurate analytical data. The new value is -167.5 ± 0.2 kcal/mole.

3. General Chemistry and Chemical Engineering

a. Conversion of Uranium Hexafluoride to Uranium Dioxide: Preparation of High-Density Particles - Studies of the method of producing dense, spheroidal uranium dioxide particles by the simultaneous reaction of uranium hexafluoride with steam and hydrogen in a fluid-bed reactor have been continued. The investigations are concerned with the effect of operating variables on particle density. Current experiments involved steam rates corresponding to 0 to 1.1 times the stoichiometric requirement, uranium hexafluoride feed rates of 17 g/min and 25 g/min, and a change in the feed-fluorine cleanup cycle (15 min/hr feed time versus the usual 30 min/hr feed time). To date, the hydrogen excesses used have been in the region of 10 to 20 times the stoichiometric requirement. The reaction temperature was 650°C. Confirming previous results, steam rates below the stoichiometric requirement resulted in lower particle densities (~8.7 g/cc, corresponding to about 80 percent of theoretical). With slightly higher than stoichiometric steam rates and a hydrogen excess of 26 times the stoichiometric requirement, the lower uranium hexafluoride feed rate (17 g/min), which in effect, results in a thinner layer of deposited material in each cycle before product is withdrawn, gave a higher density product (an increase from 9.2 to 9.5 g/cc). Using zero steam, the reduced feed time (15 min/hr), which also results in thinner layer formation per cycle, did not appear to have an effect on density. In a single run at a temperature of 700°C, a steam rate of 1.15 times the stoichiometric requirement, a hydrogen excess of 16 times the stoichiometric requirement, a uranium hexafluoride feed rate of 26 g/min, and a uranium hexafluoride

feed time of 30 min/hr, particle densities of 9.7 to 9.8 g/cc (by mercury displacement) were obtained.

Measurement of pore size distribution in uranium dioxide samples of densities varying from 8.5 to 9.8 g/cc showed that most of the pores were less than 0.4 micron in diameter.

IV. ADVANCED SYSTEMS RESEARCH AND DEVELOPMENT

A. Argonne Advanced Research Reactor (AARR)

1. Core Physics Calculations

Preliminary calculations indicate that increasing the metal-to-water ratio in the core increases the peak thermal flux per unit power. With the reference core layout, but with the fuel plate thickness increased to 0.050 in. and the coolant gap decreased to 0.030 in., the central thermal flux is calculated to be 4.9×10^{15} n/(cm^2)(sec) while the peak beam hole flux is 1.3×10^{15} n/(cm^2)(sec) at 100 Mw. When the fuel concentration is spatially varied as in the reference core, the overall maximum-to-average power ratio is 2.7 and the core cycle time is 55 days, with complete xenon override possible during the first 35 days.

Some optimization studies have been carried out to evaluate the influence of the central irradiation sample size and absorption area and the internal thermal column diameter, on neutron capture rate in the sample. At the same time the effect of void generation in the sample coolant on reactivity has been studied, since the void coefficient is positive in the internal thermal column. It has been found that a diameter of 14 cm is optimum. Complete voiding of the coolant stream within a typical sample having an absorption area of 6 cm^2 cannot yield a reactivity increment greater than 0.35% $\delta k/k$.

2. Preliminary Hazards Analyses

In the event of primary system rupture accompanied by core melting some fission products are expected to be released to the containment shell. The exclusion radius applicable to the AARR appears to be typical of water cooled reactors operating at 100 Mw.

3. Critical Experiment

The design of the components necessary to modify the ZPR-II/V critical assembly facility to perform nuclear mockup studies for the AARR is progressing. The design of the neutron source drive is being delayed pending the establishment of performance criteria on the type of source, position, and method of insertion.

An investigation to develop low cost fuel elements for the critical experiment has been initiated. Samples of depleted uranium fixed between strips of stainless steel with rubber-based glue have been tested for stability in water. No change has been detected in samples immersed in tap water at room temperature for seven weeks. However, in a test at 160°F, seal failure occurred after twelve hours. Heliarc welding of similar

sandwiches resulted in pronounced warpage. Resistance (roller) welding and electron beam welding are now being investigated.

A compact, heavy-duty control rod drive unit utilizing a stepping motor has been designed and is now being tested. The unit is powered by a synchronous motor having a permanent magnet rotor and two field windings in the stator. Steps of 1/200 revolution are achieved by reversing the current in each field alternately. Pulse counting techniques provide a convenient means for position indication.

The first drive unit constructed has now completed 3,700 raise-drop cycles with a 12-kg load. This will be continued to 10,000 cycles, to demonstrate a satisfactory dependability factor. The entire unit is only 16 x 15 x 30 cm. In its present form, two modified miniature air cylinders are used as shock absorbers. These cylinders will be replaced by standard shock absorbers so that the entire unit should be maintenance free. Design of the control circuit is in progress.

B. Direct Conversion Studies

The plasma ion production in a thermionic converter filled with cesium vapor was investigated by applying a negative voltage to the tantalum collector and grounding the emitter. The temperature of the cesium vapor was kept constant for each run and the emitter temperature was varied from about 1950°K to 2600°K.

From tabulated values for cesium pressure as a function of temperature and thermodynamic data (assuming that every cesium atom is ionized on contact with the emitter), the expression for the ion current, I(i), is given by:

$$I(i) = 5.05 \times 10^{-14}\, p \sqrt{T_{Cs}} \quad ma/cm^2 \quad ;$$

where pressure "p" is in mm Hg and T_{Cs} is the cesium vapor temperature in °K. Figure 17 shows the relationship of the emitter current densities to emitter temperatures. The applied voltages varied from -5 to -10 volts at the collector. At these negative voltages, as described in previous reports, an r-f frequency of 300 to 400 kc was observed, occasionally modulated by a frequency of about 40 kc. The observed oscillations are very different from those observed at less negative or positive collector voltages and require further investigation. The calculated values are shown for each graph by a solid circle, all other symbols represent experimental values. As may be seen, the measured values for each graph are much lower than the calculated ones for low emitter temperatures and appear to approach a saturation value at temperatures above 2200°C. Wada and Knechtli*

*Wada and Knechtli, "Generation and Application of Highly Ionized Quiescent Cesium Plasma in Steady State," Proc. IRE, Vol. 49, p. 1927 (December, 1961).

have observed similar behavior in their investigations and assumed that the ion current was suppressed by a positive space charge when the electron density fell below the ion density. However, additional work will be required to clarify this phenomena.

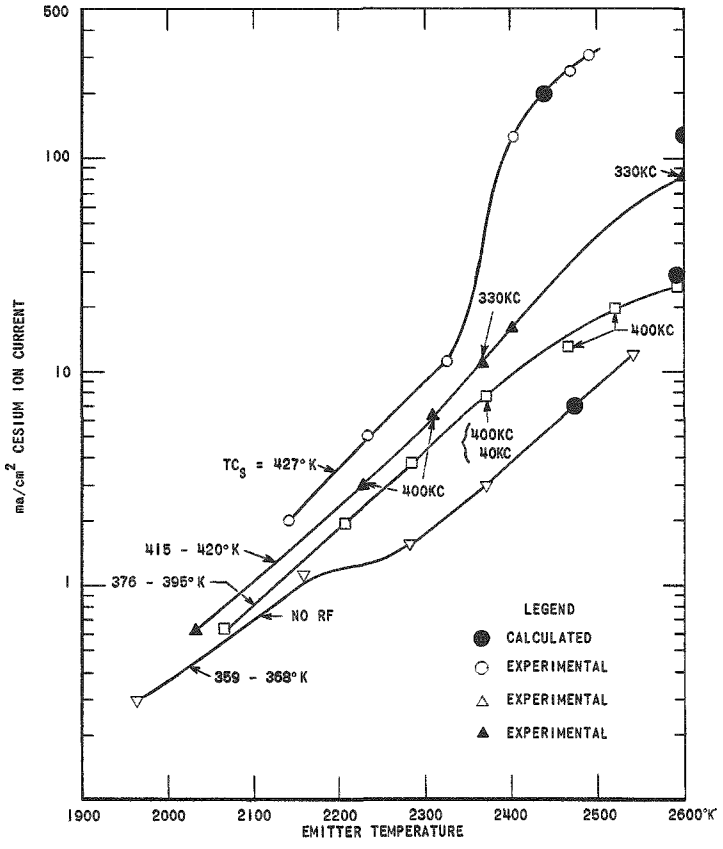

Figure 17. The curves show the experimental and calculated relationships between the emitter temperature, radiofrequency output, and the emitter current density for various cesium temperatures, T_{Cs}. The tests were conducted with -5 to -10 volts being applied to the collector and the emitter grounded.

V. NUCLEAR SAFETY

A. Thermal Reactor Safety Studies

1. Metal Oxidation and Ignition Studies

Burning curve ignition tests of eleven additional uranium alloys* (prepared by Battelle Memorial Institute) have been completed in oxygen (see Progress Report, June 1962, ANL-6580, page 52). The most outstanding observation is that the 1 atom percent bismuth-uranium alloy is somewhat less readily ignited than the copper alloys previously tested (see ANL-5974, page 24), i.e., the ignition temperature of the bismuth-uranium alloy is more than 100°C higher than that of pure uranium (595°C). Other observations were as follows:

1. The ignition temperatures of the lead and cerium alloys were slightly (about 100°C) higher than the ignition temperature of pure uranium.

2. The ignition temperatures of the rhodium, thorium, platinum, and silver alloys were similar to the ignition temperature of pure uranium.

3. The ignition temperatures of the vanadium, tantalum, and palladium alloys were slightly lower than the ignition temperature of pure uranium.

4. The ignition temperature of the titanium alloy was considerably (>100°C) lower than that of pure uranium.

Incidents reported in the literature indicate a greater pyrophoricity of uranium after irradiation. Therefore, studies of the ignition of irradiated uranium have been initiated. Small uranium pins will be enclosed in a constrainment jacket in order to avoid the complications of surface roughening, directional growth and swelling during irradiation. The constrained pins will be irradiated in MTR. Sample temperature will be limited to 300°C during irradiation.

2. Metal-Water Reaction Studies

A program is being prepared for the 704 computer to aid in the analysis of uranium-water reaction data obtained by the condenser discharge experiments and by the in-pile studies in TREAT. The equations are identical to those used previously on the analog computer for the analysis of condenser discharge results with zirconium (see ANL-6548). A term is being added to account for transient nuclear heating in TREAT runs or in a hypothetical reactor accident.

*The eleven uranium alloys included the following amounts of additive: 1 atom percent: bismuth, lead, platinum, palladium, rhodium, vanadium, tantalum, titanium, and thorium; 0.25 atom percent: silver; 400 ppm: cerium.

Studies of the reaction of solid uranium with steam by the volumetric method are continuing. In this method, steam is passed over uranium cubes supported on a thermocouple. The volume of hydrogen generated by the reaction is measured at various times. Current studies are being made with nominal 1-cm cubes of uranium containing 1 atom percent aluminum. The reaction was found to be parabolic over the range 600° to 1000°C with a tentative activation energy of 15 kcal/mole. These results were essentially identical to those found for pure uranium specimens. (See Progress Report, May 1962, ANL-6573, page 51).

In-pile studies of metal-water reactions in the TREAT facility are continuing. Two transients have been carried out with heated autoclaves in which the temperature was elevated to 285°C prior to the transient. The saturated steam within the autoclave reached a pressure of 1000 psia. The two fuel pins studied were uranium-5 wt-% zirconium-1.5 wt-% niobium. These pins received energy inputs (calculated) of approximately 100 and 200 cal/g. Hydrogen analysis revealed that 19.1 and 39.9 percent of the pins, respectively, had reacted with the water present. The extents of the reactions are significantly higher than those obtained at about 30°C and 20 psia (see ANL-6287, page 196).

Preparations have been made to conduct a series of experiments with preirradiated samples of this material.

B. Fast Reactor Safety Studies

1. Experimental Meltdown Program

Experiments are being performed in the TREAT reactor to study the mechanisms producing failure with resulting product movement in fast reactor fuel elements and to develop analytical methods for evaluating hazards to fast reactors.

a. Pre-Irradiated Sample Tests - Failure of sample elements which have previously been irradiated to appreciable levels of burnup is being investigated to study the changes in meltdown behavior produced by fission products.

The three EBR-II prototype elements subjected to clipped transients initiated with k_{ex} = 1.0% (initial asymptotic reactor period ~ 270 ms) (see ANL-6597, Progress Report for July, 1962) were examined. The tubular cladding in samples No. 1 and 2 of this group reached a temperature of 840°C and 910°C, respectively. Although the samples were badly warped, there was no evidence of cladding failure, alloying of fuel with the cladding or growth in diameter of the tube (clad). The clad in sample No. 3 reached 1120°C, and failure resulted in three places. A crack at the center of the tube permitted sodium to be ejected. Ninety-eight percent of the molten fuel from the top two-thirds of the element

was ejected against the wall of the capsule in the form of a cylinder. At a point one inch from the bottom of the element a small crack allowed some fuel to dribble out.

Twenty APDA fuel elements previously irradiated in MTR to a maximum of $\frac{3}{4}$% burnup were unloaded from their capsules. These elements are being prepared for test in the TREAT reactor. Ten elements have swollen fuel within two inches of the top. Sections of flux monitor wires from the capsules are being analyzed to verify the specified irradiation level.

b. Ceramic Fuel Element Tests - Four uranium oxide samples from the Series-XXXII transparent capsule tests were examined. Elements No. 1 and 2 were clad with niobium jackets (EBR-II size) and elements No. 3 and 4 were clad with tantalum. All samples were fueled with extruded 9.98% enriched UO_2 cylinders and bonded with Argon gas at a pressure of one atmosphere.

Sample No. 1 (maximum cladding temperature 2170°C) was warped, but did not suffer cladding failure nor was there any apparent oxide-cladding interaction. The outer cladding diameter ranged from 4.44 mm to 4.47 mm. The nominal pre-irradiation diameter was 4.42 mm. Sample No. 2 (2380°C) was also warped, and a small hole was found in the cladding 22 cm from the bottom. No fuel-cladding interaction was noted. From the rise in activity recorded at the fission gas trap in the capsule cover gas system, it could be determined that the hole was not produced during the post-transient handling. Fuel specimens from samples No. 1 and 2 showed an increase in diameter of about 0.02 mm to 0.05 mm. Cylinders from both elements took either the form of a loosely bonded oxide core surrounded by a harder cylinder comparable in appearance with unexposed oxide, or a hollow (or partially hollow) cylinder with a hard fused inner surface with drop-like oxide dribble at the bottom. Lengths of the cylinders in samples No. 1 and 2 ranged between 1.9 cm and 4 cm before the transient, but fractured and fell within the range of 1 cm to 2 cm afterward.

The cladding of sample No. 3 (2300°C) was intact, but there was a section between 10 cm and 20 cm from the bottom where the cladding was slightly bulged to about 4.75 mm diameter, and the metal surface was slightly irregular. There was no evidence of failure from the fission gas trap, but cladding was fused to the oxide. Fuel cylinders from sample No. 3 were similar in appearance to those from samples No. 1 and 2.

Fuel from sample No. 4 (maximum temperature $>$2300°C) was fused with the tantalum cladding. The cladding showed evidence of extensive melting.

XXXII

#1 #2

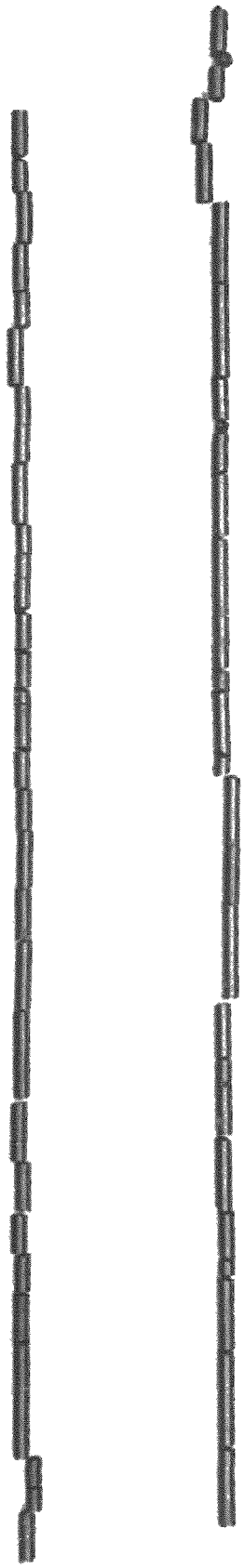

Fuel cylinders from samples No. 1 and 2 are shown in Figure 18.

2. Equipment Development

a. Large TREAT Sodium Loop - A large sodium loop is being developed as a semi-permanent installation at TREAT to provide for exposure of clusters of fuel elements at EBR-II design flow conditions. Assembly drawings and details have been established for sodium charging tanks, dump vessel, storage vessel, settling tanks, and the in-pile safety liner. Design criteria have been established for pit cover shielding, loop shielding in the TREAT basement, and loop lagging. Work has started on fabrication of components for the helium cleanup system.

b. Small (Package) Sodium Loop - The small sodium loop which is an integral experimental facility that fits into the volume of a standard TREAT fuel element, has been designed and is under construction. Drawings for the disassembly mechanism were completed. The electrical control cabinets have been assembled and wired. The fabrication of accessory equipment by Central Shops is progressing. The shipping cask was approved for purchase.

c. Instrumentation for Measuring Transient Pressures in High Temperature Sodium - Because of high sodium test temperatures and the undesirable effects of freezing and melting sodium in the loop, fast response standoffs are required to measure transient sodium pressures in loop meltdown experiments. A prototype NaK-filled bellows-sealed standoff assembly containing a miniature pressure transducer has been fabricated. Procedures were established for welding the transducer into the standoff in such a manner as to minimize the

Figure 18. Oxide Cylinder from Samples No. 1 and 2 of Series XXXII.

Note the well-formed drops apparent at the top and one-fourth of the way from the top in sample No. 2. Despite the axial cracking and the relative loss of rigidity inside the cylinders, little or no gross oxide movement was observed.

zero shift of the transducer due to distortion of its case. When the assembly was finished, the transducer output was measured as a function of static applied pressure. Zero shift was approximately 6.5%. The output was found to be linear with pressure over the rated pressure range of 0 to 10 atm gauge. Sensitivity (change in output for a given change in applied pressure) was 0.98 of that for the transducer before it was welded into the assembly and the assembly was filled with NaK. A decrease in sensitivity of 2% was calculated from the manufacturer's data on the bellows used in the standoff.

The stainless steel gas free piston engine (see Progress Report, May 1962, ANL-6573) for producing pressure pulses for use in testing transducer standoff response was finished, tested, and used for preliminary response tests on water-filled standoff tubes of simple geometry. For the tests, the engine was connected so that movement of the piston back and forth alternately opened a line connecting the test volume to a source of pressure, and then closed the line while opening a vent to the test volume. The resulting pressure-time curve at the test position was found to approximate a sine curve. Distortion from a true sine curve was similar to that which would be produced by a third harmonic having an amplitude about 30% that of the fundamental frequency. This curve was accepted as sufficiently close to the desired sine wave for testing purposes, and the engine valving was not reworked. Test frequencies over the range 20-80 cycles/sec were obtained with the engine. The frequency vs driving pressure curve followed the approximate relationship predicted theoretically of

$$\text{frequency} = K\,(\text{pressure})^{1/2}$$

over a range from 23 cps (0.2 atm gauge driving pressure) to approximately 75 cps (2.67 atm).

3. Theoretical Studies

a. Machine Calculation of Transient Heat Transfer - An IBM-704 code (1528/RE) has been developed in Fortran language, to calculate analytically the transient temperatures in a cylindrical rod with uniform and constant internal heat generation, cooled on the surface.

Temperatures are given by the infinite series[1]

$$T(r,t) = T_0 + \frac{QR^2}{4K}\left[1-\left(\frac{r}{R}\right)^2 - \frac{2}{Rh}\right] - \frac{2hQ}{RK}\sum_{n=1}^{\infty} e^{-\kappa t\alpha_n^2}\frac{J_0(r\alpha_n)}{\alpha_n^2(h^2+\alpha_n^2)J_0(R\alpha_n)} \quad (1)$$

[1] Carslaw and Jaeger, Conduction of Heat in Solids, p. 205 (1959).

where

$T(r,t)$ = temperature at radius r, and time t

T_0 = initial temperature, independent of radius

Q = rate of heat generation per unit volume

R = outer radius of cylindrical rod

K = thermal conductivity of rod material

h = boundary film coefficient/thermal conductivity

κ = thermal diffusivity of rod material

and the α_n are the positive eigenvalues of $\alpha J_1(R\alpha) - hJ_0(R\alpha) = 0$.

The solution of this problem (Eq. 1) also requires that the coolant temperature be equal to the pin initial temperature T_0 for all time t.

This code is being used to check analytically the results obtained by numerical methods using the more complicated heat transfer code ARGUS.

b. Heat Transfer Calculations of TREAT Meltdown Experiments on EBR-II - Work continued using the RE 147 CYCLOPS heat transfer code to calculate temperature distributions for EBR-II samples undergoing transient power excursions in TREAT (see Monthly Progress Reports, ANL-6473, ANL-6485, and ANL-6573). The most recent analysis was a study of whether or not the fuel-cladding interface temperature attained the temperature for violent failure (1015°C) before coolant bulk boiling began. The effects of coolant velocity, fuel enrichment, and the initial TREAT excess reactivity have been previously surveyed. The hydrodynamics and heat transfer characteristics associated with bulk boiling of the coolant and movement of the fuel are very complex and more advanced techniques will be required to explain the behavior of these systems

By comparing the time that bulk boiling begins with the time the failure occurs, it is possible to obtain an insight into the conditions existing at the time of element failure and the environment "viewed" by meltdown products as they begin their movement from the element.

Qualitatively, it appears that once bulk boiling begins, it will continue and lead to failure of the element due to stoppage of the coolant flow. Hence, calculations that boiling is reached before failure temperatures are attained would imply that in practice failure occurs more quickly after boiling than indicated by the CYCLOPS code or that failure could occur whether or not it is predicted to occur after boiling is indicated by

the CYCLOPS temperature output. It has not been determined under what conditions bulk boiling would cease once it has started.

As an example, for an initial TREAT k_{ex} = 1.6% (period of about 100 ms) and a sample enrichment of nearly 3% the calculations indicated that bulk boiling would occur before failure temperatures were reached up to a coolant velocity of about 6.1 m/sec. However, for the same enrichment, but initial k_{ex} = 2.4% (period of about 60 ms), failure would occur before bulk boiling in all cases.

Work is continuing to develop the theory of conditions subsequent to the onset of boiling.

VI. PUBLICATIONS

Papers

CORRELATION FOR TWO-PHASE FLOW
John F. Marchaterre and Barton M. Hoglund
Nucleonics 20, No. 8, p. 142 (August, 1962)

RESONANCE INTEGRALS FOR GOLD AND INDIUM FOILS
Charles N. Kelber
Nucleonics 20, No. 8, p. 162 (August 1962)

OPTICAL MODEL FRINGE ABSORPTION AND THE NEUTRON STRENGTH FUNCTION
P. A. Moldauer
Physical Review Letter 9, No. 1, pp. 17-19 (July 1, 1962).

Book Review of AN INDEX OF MATHEMATICAL TABLES and GUIDE TO TABLE IN MATHEMATICAL STATISTICS
Henry C. Thacher, Jr.
Science 137, No. 3527, p. 332 (August 3, 1962)

SENSITIVITY OF PRESSURE TRANSDUCERS TO TRANSIENT NEUTRON AND GAMMA RADIATION
J. F. Boland, R. D. DeForest, R. O. Ivins, F. S. Kirn, H. Lawroski and R. C. Liimatainen
Trans. Am. Nuclear Soc. 5 (1), 186 (1962).

SINTERING OF URANIUM MONOCARBIDE PRECIPITATED FROM LIQUID METAL MEDIA
T. R. Johnson, G. D. White, J. Handwerk and R. K. Steunenberg
Trans. Am. Nuclear Soc. 5 (1), 243 (1962).

THE HIGH TEMPERATURE BEHAVIOR IN WATER OF URANIUM DIOXIDE CORE, STAINLESS STEEL-304 CLAD FUEL PINS DURING REACTOR TRANSIENTS
R. C. Liimatainen, R. O. Ivins and D. C. Hill
Trans. Am. Nuclear Soc. 5 (1), 234 (1962).

SPECTROPHOTOMETRIC DETERMINATION OF IRON IN URANIUM-FISSION ELEMENT ALLOYS
J. J. McCown and D. E. Kudera
Anal. Chem. 34, 870 (1962) Letter

THE CRYSTAL STRUCTURES OF TiCd AND Ti_2Cd
R. V. Schablaske, B. S. Tani and M. G. Chasanov
Trans. Met. Soc. AIME 224, 867 (1962).

CERTIFICATION OF ALGORITHM 37. TELESCOPE 1 (K. A. Brons, Comm. ACM., March, 1961)
Henry C. Thacher, Jr.
Comm. ACM, Vol. 5, No. 8, p. 438 (August, 1962)

CERTIFICATION OF ALGORITHM 57. BER OR BEI FUNCTION (John R. Herndon, Comm. ACM, April, 1961)
Henry C. Thacher, Jr.
Comm. ACM, Vol. 5, No. 8, p. 438 (August, 1962)

CERTIFICATION OF ALGORITHM 18. RATIONAL INTERPOLATION BY CONTINUED FRACTIONS (R. W. Floyd, Comm. ACM, September, 1960)
Henry C. Thacher, Jr.
Comm. ACM, Vol. 5, No. 8, p. 437 (August, 1962)

ANL Reports

ANL-6516 ANNUAL REPORT FOR 1961, METALLURGY DIVISION

ANL-6540 RADIATION PROBLEMS ASSOCIATED WITH THE HANDLING OF THE ACTINIDE ELEMENTS
Martin J. Steindler

ANL-6543 CHEMICAL ENGINEERING DIVISION SUMMARY REPORT, January, February, March, 1962

ANL-6548 STUDIES OF METAL-WATER REACTIONS AT HIGH TEMPERATURES III. EXPERIMENTAL AND THEORETICAL STUDIES OF THE ZIRCONIUM-WATER REACTION
Louis Baker, Jr. and Louis C. Just

ANL-6559 FEASIBILITY OF Pu^{239}-U^{235}-FUELED CORES TO PREDICT Pu^{239}-FUELED CORE DIMENSIONS
D. Meneghetti and H. Ishikawa

ANL-6570 k CALCULATIONS FOR 22 ZPR-III FAST REACTOR ASSEMBLIES USING ANL CROSS-SECTION SET 635
W. G. Davey

ANL-6581 A STUDY OF VAPOR CARRYUNDER AND ASSOCIATED PROBLEMS
Michael Petrick